PERGAMON

Applied Geochemistry 14 (1999) 581–606

Applied Geochemistry

Limestone drains to increase pH and remove dissolved metals from acidic mine drainage

Charles A. Cravotta III [a,*], Mary Kay Trahan [b]

[a] *Hydrologist, U.S. Geological Survey, 840 Market Street, Lemoyne, PA 17043, USA*
[b] *ECO Associate and Engineer, Wallis Engineering, 119 E. 8th Street, Vancouver, WA 98660, USA*

Received 22 December 1997; accepted 3 July 1998
Editorial handling by D.D. Runnells

Abstract

Despite encrustation by Fe and Al hydroxides, limestone can be effective for remediation of acidic mine drainage (AMD). Samples of water and limestone ($CaCO_3$) were collected periodically for 1 a at 3 identical limestone-filled drains in Pennsylvania to evaluate the attenuation of dissolved metals and the effects of pH and Fe- and Al-hydrolysis products on the rate of $CaCO_3$ dissolution. The influent was acidic and relatively dilute (pH < 4; acidity < 90 mg) but contained 1–4 mg·L^{-1} of O_2, Fe^{3+}, Al^{3+} and Mn^{2+}. The total retention time in the oxic limestone drains (OLDs) ranged from 1.0 to 3.1 hr. Effluent remained oxic (O_2 > 1 mg·L^{-1}) but was near neutral (pH = 6.2–7.0); Fe and Al decreased to less than 5% of influent concentrations. As pH increased near the inflow, hydrous Fe and Al oxides precipitated in the OLDs. The hydrous oxides, nominally $Fe(OH)_3$ and $Al(OH)_3$, were visible as loosely bound, orange-yellow coatings on limestone near the inflow. As time elapsed, $Fe(OH)_3$ and $Al(OH)_3$ particles were transported downflow. The accumulation of hydrous oxides and elevated pH (> 5) in the downflow part of the OLDs promoted sorption and coprecipitation of dissolved Mn, Cu, Co, Ni and Zn as indicated by decreased concentrations of the metals in effluent and their enrichment relative to Fe in hydrous-oxide particles and coatings on limestone. Despite thick (~1 mm) hydrous-oxide coatings on limestone near the inflow, $CaCO_3$ dissolution was more rapid near the inflow than at downflow points within and the OLD where the limestone was not coated. The high rates of $CaCO_3$ dissolution and $Fe(OH_3)$ precipitation were associated with the relatively low pH and high Fe^{3+} concentration near the inflow. The rate of $CaCO_3$ dissolution decreased with increased pH and concentrations of Ca^{2+} and HCO_3^- and decreased Pco_2. Because overall efficiency is increased by combining neutralization and hydrolysis reactions, an OLD followed by a settling pond requires less land area than needed for a two-stage treatment system consisting of an anoxic limestone drain and oxidation-settling pond or wetland. To facilitate removal of hydrous-oxide sludge, a perforated-pipe subdrain can be installed within an OLD.

1. Introduction

Acidic mine drainage (AMD) is a major source of water contamination in coal- and metal-mining districts worldwide (Powell, 1988). In the northern Appalachian Plateau of the eastern United States (U.S.A.), discharges from abandoned coal mines affect more than 8000 km of streams and associated ground water (Boyer and Sarnoski, 1995). The majority of the affected streams are in Pennsylvania, where approximately half the discharges from bituminous and anthracite coal mines are acidic, having a pH < 5 (Brady et al., 1997). The AMD typically contains elevated concentrations of dissolved and particulate Fe and dissolved SO_4^{2-} produced by the oxidation of

* Corresponding author.

0883-2927/99/$ - see front matter
PII: S0883-2927(98)00066-3

pyrite (FeS_2):

$$FeS_2 + 3.5\ O_2 + H_2O \longrightarrow Fe^{2+} + 2\ SO_4^{2-} + 2\ H^+ \quad (1)$$

$$Fe^{2+} + 0.25\ O_2 + H^+ \longrightarrow Fe^{3+} + 0.5\ H_2O \quad (2)$$

$$Fe^{3+} + 3\ H_2O \longrightarrow Fe(OH)_3\ (s) + 3\ H^+ \quad (3)$$

Despite the stoichiometry indicated by Eq. (1), the molar ratio of dissolved SO_4^{2-} to Fe $[SO_4^{2-}]/([Fe^{2+}] + [Fe^{3+}])$ in AMD containing oxygen (O_2) commonly exceeds 2 because of the relatively high solubility of SO_4^{2-} and low solubility of Fe^{3+}, which tends to precipitate as $Fe(OH)_3$ and related solids[1] in moderately acidic to neutral solutions ($3.5 \leq pH \leq 7$). Concentrations of Mn^{2+}, Al^{3+} and other solutes in AMD commonly are elevated due to aggressive dissolution of carbonate, oxide and aluminosilicate minerals by acidic water along flow paths downflow from oxidizing pyrite (Cravotta, 1994; Blowes and Ptacek, 1994).

AMD commonly develops where the carbonate minerals, calcite ($CaCO_3$) and dolomite ($CaMg(CO_3)_2$), are absent or deficient relative to pyrite in coal overburden (Brady et al., 1994). Dissolution of calcite, which is the principal component of limestone, can neutralize acidity and increase pH and concentrations of alkalinity ($HCO_3^- + OH^-$) and Ca^{2+} in mine water by the following reactions:

$$CaCO_3\ (s) + 2H^+ \leftrightarrow Ca^{2+} + H_2CO_3^* \quad (4)$$

$$CaCO_3\ (s) + H_2CO_3^* \leftrightarrow Ca^{2+} + 2\ HCO_3^- \quad (5)$$

$$CaCO_3\ (s) + H_2O \leftrightarrow Ca^{2+} + HCO_3^- + OH^- \quad (6)$$

where $[H_2CO_3^*] = [CO_2\ (aq)] + [H_2CO_3^0]$ (Plummer et al., 1979; Stumm and Morgan, 1996). The overall rate of calcite dissolution depends on the pH, the partial pressure of CO_2 (Pco_2), and the activities of H_2O, Ca^{2+}, and HCO_3^- near the calcite surface (Plummer et al., 1979; Morse, 1983; Arakaki and Mucci, 1995). Generally, the overall rate of calcite dissolution will decrease as the pH and activities of Ca^{2+} and HCO_3^- increase and the Pco_2 decreases.

Use of limestone for neutralization of AMD in surficial environments has been limited because of its low solubility and slow dissolution rate relative to other alkaline reagents and decreased efficiency of neutralization associated with its "armoring" (strong adhesion and complete pacification by encrustation) with Fe^{3+} and Al^{3+} compounds (Hill and Wilmoth, 1971; Lovell, 1972). Recently, however, passive-treatment systems that use limestone to neutralize AMD have become popular because they are relatively inexpensive to construct and maintain (Hedin et al., 1994a). Treatment systems including anoxic limestone drains (Turner and McCoy, 1990; Brodie et al., 1991; Hedin and Watzlaf, 1994; Hedin et al., 1994b), open limestone channels (Ziemkiewicz et al., 1997), and limestone diversion wells (Arnold, 1991; Cram, 1996) have been demonstrated to neutralize AMD and downstream water in mined watersheds in the eastern U.S.A. Each of these systems has limitations in effectiveness and applicability.

Anoxic limestone drains (ALDs), which have been designed to avoid armoring, are particularly effective for generation of alkalinity (Hedin et al., 1994b). In its simplest form, an ALD is a buried, limestone-filled trench that intercepts AMD before its exposure to atmospheric O_2. Retaining CO_2 within an enclosed ALD can enhance calcite dissolution and alkalinity production by Eq. (5). By this mechanism, a greater quantity of alkalinity can be generated in an ALD, which is enclosed to minimize gas flux, compared to systems such as limestone channels or diversion wells that are open to the atmosphere. After treatment by an ALD, effluent is exposed to the atmosphere, and solid $Fe(OH)_3$ is produced by the oxidation of Fe^{2+} to Fe^{3+} by Eq. (2) and the consequent hydrolysis of Fe^{3+} by Eq. (3) or by

$$Fe^{3+} + 3\ HCO_3^- \longrightarrow Fe(OH)_3\ (s) + 3\ CO_2 \quad (7)$$

Excluding O_2 from contact with the mine water in an ALD minimizes the potential for in situ precipitation of $Fe(OH)_3$. The precipitation of $Fe(OH)_3$ and various other OH and/or SO_4 compounds of Fe^{3+}, Al^{3+} and possibly Ca^{2+}, within an ALD can armor the limestone surface, decreasing the rate and extent of limestone dissolution and alkalinity production (Watzlaf et al., 1992; Hedin and Watzlaf, 1994; Aschenbach, 1995; Robbins et al., 1997). Furthermore, the accumulation of precipitated compounds can decrease the porosity and permeability of limestone-treatment systems (Watzlaf et al., 1994; Robbins et al., 1996). Hence, design criteria for ALDs as proposed by Hedin et al. (1994a) and Hedin and Watzlaf (1994) generally are conservative with respect to influent chemistry (requirement of <1 mg of dissolved O_2, Fe^{3+} or Al^{3+}) and sizing (prolonged residence time) to ensure "maximum" alkalinity production over the life of an ALD.

[1] Hereafter, $Fe(OH)_3$ indicates the hydrous Fe-oxide and SO_4 compounds that together form ochres in AMD environments, including $Fe(OH)_3$ or ferrihydrite (nominally $Fe_5HO_8{\cdot}4H_2O$), goethite (α-FeOOH), schwertmannite ($Fe_8O_8(OH)_6SO_4$), and jarosite ($(H,K,Na)Fe_3(SO_4)_2(OH)_6$) (Taylor and Schwertmann, 1978; Ferris et al., 1989; Murad et al., 1994; Bigham et al., 1996).

Stringent requirements for low concentrations of O_2, Fe^{3+} and Al^{3+} in AMD make ALDs inappropriate for treatment of oxic or highly mineralized water, which commonly occurs in mined areas (Wood, 1996; Rose and Cravotta, 1998). Thus, variations on the basic ALD design have been proposed. One alternative uses pretreatment through a compost layer to decrease concentrations of dissolved O_2, Fe^{3+} and Al^{3+} in the mine water to acceptable levels before routing the water through a limestone layer (Kepler and McCleary, 1994). Nevertheless, short-term laboratory studies (<2 a) indicate that limestone alone can be as effective as this layered system for neutralization of oxic mine water containing moderate concentrations of Fe^{3+} and Al^{3+} (10–20 $mg{\cdot}L^{-1}$) (Watzlaf, 1997; Sterner et al., 1998). This variation on the ALD design is essentially an oxic limestone drain (OLD). In an enclosed OLD, oxidation and hydrolysis reactions will not be prevented (Eq. (2), Eq. (3) and Eq. (7)). If sufficiently rapid flow rates can be attained, the solid hydrolysis products may be transported through the OLD. Despite potential for armoring and clogging, the hydrous oxides may be effective for the sorption of dissolved Mn^{2+} and trace metals (Anderson and Rubin, 1981; Coston et al., 1995; Smith et al., 1998). Additionally, the in situ production and retention of H^+ and CO_2 in an OLD may promote limestone dissolution (Eq. (4) and Eq. (5)). However, the processes and function of OLDs under field conditions have not been evaluated previously.

To investigate hydrogeochemical processes within limestone drains under oxic conditions, the U.S. Geological Survey (USGS) constructed 3 experimental OLDs in 1995 to treat acidic drainage from an abandoned coal mine. The flow rate and initial dissolved O_2 concentration of the influent to one or more of the OLDs were varied to determine any effects on the rates of dissolution and precipitation reactions and the transport of reaction products through the OLDs. Monitoring was conducted for 1 a during 1995–96. Water and rock samples were collected and analyzed to explain changes in water chemistry within the OLDs as a result of oxygenation, dissolution, precipitation and sorption reactions. This report evaluates effects of pH, dissolved O_2, solute concentrations, hydrolysis of Fe^{3+} and Al^{3+}, and flow rates (residence time) on limestone dissolution and metals transport within these experimental OLDs.

2. Methodology

2.1. Design of experimental limestone drains

In February 1995, 3 identical OLDs were constructed in parallel to treat AMD seeping from and the collapsed entrance to the Orchard Mine drift in the Southern Anthracite Coalfield in E-central Pennsylvania (lat. 40°36′26″ N, long. 76°25′30″ W). The 3 OLDs were installed side by side in a horizontal, 4-m wide by 30-m long trench to depths of 1–2 m (Fig. 1). Each OLD was constructed using 0.79-m inside-diameter (ID) corrugated steel culvert pipe that was split lengthwise to form a semicircular trough that was 24.4 m long, with a cross-sectional area of 0.244 m^2. After lining the trough with vinyl sheeting (0.051-cm thick), a total of 12 700 kg of tabular, 3-cm minimum width by 10-cm maximum length, limestone fragments (97% $CaCO_3$) was placed in each OLD. The vinyl liner was wrapped over the top of the limestone before backfilling with excavated soil to the original land-surface grade. Water was first routed through the system on March 15, 1995, after sufficient time had elapsed for the caulked seams to cure.

A wooden dam was installed across the debris-filled mine opening to stabilize the static water level and to minimize aeration. Approximately 15 m of 5-cm ID polyvinyl chloride (PVC) pipe was used to transmit the mine water through the dam to the 3 OLDs. At the inflow to the drains, plumbing valves and a static mixer, consisting of a 30-cm ID standpipe filled with polyethylene trickling media, enabled aeration (pure O_2), deaeration (N_2 sparging), or no pretreatment of the inflow to all 3 or to only one of the drains (Fig. 1). During the initial part of the study, raw mine water and compressed N_2 or O_2 gas were introduced at the bottom of the static mixer (about 1 m below ground level) and flowed upward 2.1 m through the trickling media to promote gas exchange before the water was diverted into the OLD(s). A one-way valve at the top of the static mixer allowed excess gas to escape. The outflow pipe from each OLD consisted of a U-shaped trap and riser that extended about 0.2 m above the top of the limestone to ensure continuous inundation of the limestone and to minimize airflow into the drains.

For water and rock sampling, capped, 5-cm ID PVC pipes were installed within the OLDs at ports 1.5, 3, 6.1, 12.2 and 18.3 m downflow from the inflow (Fig. 1). Sampling access ports also were installed at the inflows to the static mixer and to each OLD. For water sampling, flexible vinyl tubing was extended down through a hole in each capped pipe to mid-depth within each OLD, 0.2 m from the bottom of the drains. To prevent airflow through the tubing, removable clamps or plugs were used. To prevent large particles from entering the tubing, polyester filter fabric was wrapped around the open pipe and tubing within the drain.

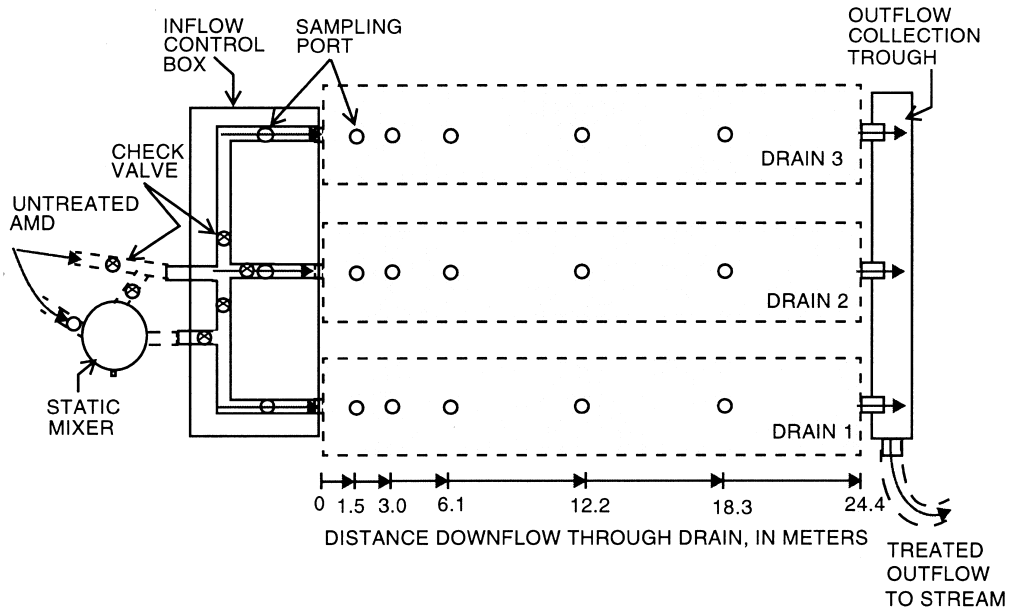

Fig. 1. Schematic design of the oxic limestone drains (OLDs) at the Orchard Overflow in the upper part of the Swatara Creek watershed, E. central Pennsylvania.

2.2. Sampling and analytical methods

Water samples from inflow, outflow, and intermediate points within each OLD were routinely collected at 3- to 4-week intervals during March 1995–March 1996, except when access was blocked by deep snow cover during December and January. Water samples were retrieved by use of a peristaltic pump while maintaining a constant flow rate through each OLD. Samples of untreated AMD also were collected at an adjacent overflow ditch, which bypassed the OLDs (untreated control). The volumetric flow rate was measured by recording the time to collect a known volume of water at the OLD outflow and overflow-ditch sampling points.

Temperature, dissolved O_2 (DO), specific conductance (SC), redox potential (Eh), and pH of water samples were measured electrometrically in the field according to methods of Wood (1976) by diverting water through a glass flow cell. Before conducting sample measurements, all meters were calibrated in the field with appropriate electrodes and standards that had been thermally equilibrated to sample temperatures. Eh was measured with a combination Pt and Ag/AgCl electrode, checked with Zobell's solution, and corrected to 25°C according to methods of Nordstrom (1977).

Water samples were split into subsamples and stored in sample-rinsed polyethylene bottles, on ice, until laboratory analysis. Two unfiltered subsamples for analysis of (1) acidity and alkalinity and (2) anions were capped leaving no head space. A third subsample for analysis of "dissolved" cations and silica was filtered through a 0.45-μm pore-size nitrocellulose capsule filter, transferred to an acid-rinsed bottle, and preserved with HNO_3 to pH <2. The fourth subsample for analysis "total" metals was not filtered and was preserved with HNO_3 to pH <2. Because sampling tubes within the OLDs were covered by a filter fabric, the whole-water sample for total metals was collected only at the inflow, outflow, and overflow.

Alkalinity and acidity (H^+ + hydrolyzable metals)[2] for unfiltered samples usually were titrated in the field at ambient temperature with H_2SO_4 (1.6 and 0.16 N) and NaOH (0.1 N) to pH 4.5 and 8.3 endpoints, respectively, using methods of Fishman and Friedman (1989). However, on some occasions, generally within 24 hr after sample collection, the alkalinity and/or acidity titrations were completed in the USGS Laboratory in Lemoyne, Pa. Field and laboratory alkalinity or acidity on split samples were indistinguishable.

[2] Acidity, the opposite of alkalinity, measures the base-neutralizing capacity of a solution. Acidity can be estimated as the sum of concentrations of hydrolyzable cations and their complexes, including H^+, Fe^{3+}, Fe^{2+}, Al^{3+} and Mn^{2+}, in milliequivalents per liter (meq L^{-1}), which is multiplied by 50 to obtain results as milligrams per liter (mg·L^{-1}) $CaCO_3$ (Rose and Cravotta, 1998; Hedin et al., 1994a).

Concentrations of SO_4, SiO_2, Ca, Mg, Na, Fe, Mn, Al and selected trace metals (Ag, Ba, Be, Cd, Cr, Co, Cu, Li, Mo, Ni, Pb, Sr, V, Zn)[3] were determined at the USGS National Water Quality Laboratory in Arvada, Co., using methods of Fishman and Friedman (1989). Anions were analyzed by ion chromatography (IC). Silica and cations, except for Al, were analyzed by inductively coupled Ar plasma atomic emission spectroscopy (ICP). Concentrations of Al were analyzed by direct current Ar plasma atomic emission spectroscopy (DCP). Charge imbalances routinely were less than 5% relative to the mean of cation and anion equivalents. Duplicates and USGS Standard Reference Water Samples that were submitted with each set of samples indicated overall precision and accuracy within 5% for all constituents. Deionized water blanks and filter blanks routinely indicated concentrations below detection for all analytes.

Activities of aqueous species, Pco_2, and mineral saturation indices were calculated using the WATEQ4F computer program (Ball and Nordstrom, 1991). The saturation index (SI) provides a basis for evaluating the potential for dissolution or precipitation of a solid phase by the water (Stumm and Morgan, 1996). Values of SI that are negative (< -0.1), approximately zero (± 0.1), or positive (> 0.1) indicate the water is undersaturated, saturated, or supersaturated, respectively, with the solid phase. If undersaturated, the water can dissolve the solid phase. If supersaturated, the water cannot dissolve the solid phase but can potentially precipitate it.

In March 1995, sawed pieces of limestone (1–2 cm thick by 3–4 cm width "slabs") and cleavage rhombs of calcite (Iceland spar) were measured for weight, porosity, and geometric surface dimensions (thickness, width, length) and then were suspended with braided nylon chord to be immersed within the OLDs. In August 1995 and March 1996, the limestone slabs and calcite rhombs were retrieved and remeasured to determine the rate of limestone dissolution at a particular location and the chemistry and mineralogy of any encrustation. The dissolution rate was normalized with respect to the geometric surface area of the sample so that the field results could be compared with rate estimates from published laboratory experiments. Encrustations on the limestone and calcite samples were detached by gently rinsing the samples with deionized water. The detached material was dried at 180°C, weighed, and dissolved in a 50% solution of 1:1 HCl and HNO_3 for analysis of "total" metals. Additionally, hydrous oxides collected from the OLDs in 1997 were analyzed qualitatively for mineralogy and chemistry by X-ray diffractometry (XRD) and X-ray energy dispersive spectroscopy (EDS), respectively.

[3] Hereafter, the use of an elemental or molecular formula without charge notation indicates the total analytical concentration in solution without regard to valence or the possible existence of ion pairs or other complex species.

2.3. Determination of residence time

Residence time (t_R) and porosity (n) within the OLDs were determined by several methods. First, on March 15, 1995, when OLD–1 was filled at a constant flow rate (Q) of 6.3 $L \cdot min^{-1}$, approximately 2 hr were required to produce outflow. Accordingly, the t_R was approximately 2 hr at that flow rate, and the volume of water-filled voids (V_V) was computed to be approximately 756 L ($= 120$ min·6.3 $L \cdot min^{-1}$). Second, on March 26, 1996, t_R of OLD-1 was measured using a tracer test. While maintaining a constant flow rate ($Q = 12.1$ $L \cdot min^{-1}$), pure O_2 gas was introduced in the static mixer for 15 min, producing a pulse of influent supersaturated with O_2 (> 20 $mg \cdot L^{-1}$). Despite dispersion as the pulse flowed through the drain, measurements revealed a plume of oxygenated water at successive downflow points, with the peak DO concentration reaching 12.2 m in 34.5 min, 18.3 m in 46.5 min, and 24.4 m at the outflow in 66.5 min (average velocity 0.37 $m \cdot min^{-1}$). Accordingly, for the flow rate of the test, t_R at the outflow was 1.1 hr, and V_V was computed to be 805 L ($= 12.1$ $L \cdot min^{-1} \cdot 66.5$ min), which is in agreement with the first estimate. Because the 3 OLDs were constructed to be identical, each having a total volume (V_T) of 5.95 m^3 ($= 24.4$ m·0.244 m^2), the porosity of the OLDs was computed to be 0.14 ($= 0.805$ $m^3/5.95$ $m^3 = V_V/V_T$). This "field" porosity estimate is comparable with an estimate of 0.19 ($= (V_T - V_S)/V_T$) computed as the difference between the total volume of the drain and the estimated volume of the stone determined using the measured density of the stone ($\rho_S = 2.63$ $g \cdot cm^{-3}$; $V_S = 12\,727$ kg/2630 $kg \cdot m^{-3}$). However, these porosity estimates are significantly lower than the "laboratory" value of 0.5 measured for hand-picked limestone fragments in a 19-L bucket (as determined for this study and by Hedin and Watzlaf, 1994). Although porosities could range widely among different limestone drains because of differences in compaction and sorting of limestone fragments, low porosities in the field are likely to result from compaction of mixed-size, tabular limestone fragments; rough or flexible outside walls; and the accumulation of secondary minerals on and between limestone fragments.

Finally, data for porosity and flow rate were used to compute the residence time for water at each point sampled and over the range of flow rates evaluated. According to Darcy's equation (Freeze and Cherry, 1979), the velocity of flow through a porous medium is

$$v = Q/(A \cdot n), \quad (8)$$

where Q is the volumetric flow rate, A is the cross-sectional area perpendicular to flow, and n is the porosity. By substituting $v = L/t_R$, where L is the distance along the flow path, and rearranging, t_R and at any distance from the inflow could be determined for a given Q (Fig. 2), assuming constant values for $A = 0.244$ m^2 and $n = 0.14$:

$$t_R = (L \cdot A \cdot n)/Q \quad (9)$$

Note that t_R is proportional to downflow distance and the numerator of Eq. (9) is the void volume at that distance.

Residence times also were estimated using another form of Darcy's equation (Hedin and Watzlaf, 1994):

$$t_R = (M_S \cdot n/\rho_b)/Q, \quad (10)$$

where M_S is mass of limestone and is ρ_b the bulk density of the limestone. The numerator of Eq. (10) also indicates the void volume; however, assuming a constant particle density (ρ_S), bulk density decreases as porosity increases ($n = 1 - \rho_b/\rho_s$; Freeze and Cherry, 1979). Thus, the effect on t_R from the interdependence of n and ρ_b is magnified by Eq. (10). Eq. (9) and Eq. (10) produce the same result for t_R at the outflow of drains, using measured values of $L = 24.4$ m, $A = 0.244$ m^2, $n = 0.14$, $M_S = 12\,727$ kg, and $\rho_b = 2140$ kg·m^{-3}. However, if values of $n = 0.5$ and $\rho_b = 1600$ kg·m^{-3} assumed by Hedin and Watzlaf (1994) are used in Eq. (10), estimates of t_R are 5 times greater than measured.

3. Results and discussion

3.1. Hydrochemical trends

During March 1995–March 1996, the untreated AMD influent had ranges of pH = 3.2–3.8, SC = 410–710 μS·cm^{-1}, and concentrations of DO = 1.3–3.4 mg·L^{-1}, acidity = 31–85 mg·L^{-1}, SO_4 = 130–300 mg·L^{-1}, and dissolved Al, Fe, and Mn, in order of increasing abundance, of 0.6–4 mg·L^{-1} (Table 1). The dissolved Fe^{3+} concentration in the influent ranged from 0 to 90% and averaged about 26% of the total dissolved Fe concentration (Table 1). Rock, wood, and pipe surfaces exposed to the AMD were coated by rust-colored hydrous Fe(III)-oxides that were identified as schwertmannite and goethite (J. M. Bigham, 1997, written commun.). The AMD hosted numerous microorganisms, including rod-shaped bacteria, fungi, and

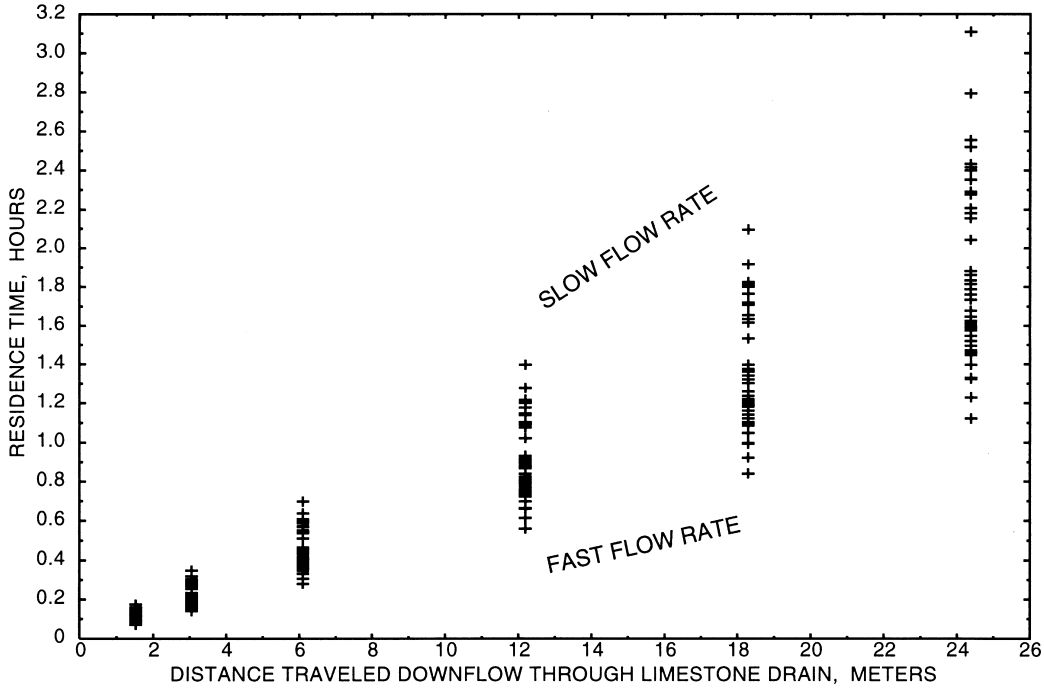

Fig. 2. Relation between calculated residence time and distance traveled through OLDs 1, 2, and 3 for the range of flow rates evaluated. Residence time computed as distance times cross-sectional area (0.244 m^2) times porosity (0.14) divided by volumetric flow rate (m^3·hr^{-1}).

Table 1. Summary of measured compositions of water at inflow, overflow, and outflow of the 3 oxic limestone drains at Orchard Mine, Pennsylvania, March 1995–March 1996

Parameter or constituent[a]	Untreated influent			Untreated overflow[b]			Treated effluent from limestone drains[b]		
	N	Median	Minimum/maximum	N	Median	Minimum/maximum	N	Median	Minimum/maximum
Discharge, m^3/d	16	29.9	(23.4 / 44.8)	9	57.7	(16.4 / 150.9)	48	29.9	(23.4 / 44.8)
Temperature, °C	17	10.7	(8.3 / 12.6)	16	12.9	(5.7 / 15.0)	49	10.7	(7 5 / 12.4)
Eh, volts	17	0.70	(0.49 / 0.77)	16	0.67	(0.33 / 0.73)	49	0.40	(0.31 / 0.52)
Spec. Cond., µS/cm	17	550	(410 / 710)	16	550	(410 / 590)	49	610	(390 / 790)
Dissolved O_2	17	2.2	(1.3 / 3.4)	14	9.7	(1.8 / 17.8)	49	2.9	(1.8 / 19.5)
pH, units	17	3.5	(3.2 / 3.8)	16	3.5	(3.3 / 5.0)	49	6.6	(6.2 / 7.0)
Alkalinity as $CaCO_3$	17	0	(0 / 0)	15	0	(0 / 0)	48	108	(55 / 136)
Acidity as $CaCO_3$	14	63	(31 / 85)	12	34	(23 / 51)	27	0	(0 / 26)
Net alkalinity as $CaCO_3$	14	−63	(−85 / −31)	11	−33	(−41 / −23)	27	113	(67 / 136)
Ca	10	29.0	(16.0 / 39.0)	5	29.0	(17.0 / 49.0)	33	79.0	(49.0 / 110.0)
Mg	10	26.0	(16.0 / 35.0)	5	27.0	(16.0 / 35.0)	33	26.0	(16.0 / 35.0)
Na	10	0.8	(0.8 / 0.9)	5	0.9	(0.8 / 0.9)	33	0.8	(0.7 / 1.0)
SO_4	10	215	(130 / 300)	5	220	(140 / 290)	33	200	(130 / 290)
SiO_2	10	9.6	(9.2 / 10.0)	5	10.0	(9.3 / 10.0)	33	9.4	(7.7 / 10.0)
Al	10	0.93	(0.73 / 1.50)	5	1.10	(0.90 / 1.30)	33	0.04	(0.02 / 0.09)
Al, total	10	0.89	(0.70 / 1.30)	5	1.20	(0.82 / 1.30)	32	0.08	(<0.01 / 0.40)
Ag	10	<0.001	(<0.001 / 0.004)	5	<0.001	(<0.001 / 0.002)	33	<0.001	(<0.001 / <0.002)
Ba	10	0.019	(0.019 / 0.024)	5	0.021	(0.021 / 0.022)	33	0.019	(0.014 / 0.021)
Be	10	0.001	(<0.001 / 0.003)	5	0.002	(<0.001 / 0.002)	33	<0.001	(<0.001 / 0.001)
Cd	10	<0.001	(<0.001 / 0.001)	5	<0.001	(<0.001 / 0.001)	33	<0.001	(<0.001 / 0.003)
Cr	10	<0.005	(<0.005 / <0.005)	5	<0.005	(<0.005 / <0.005)	33	<0.005	(<0.005 / <0.005)
Co	10	0.093	(0.072 / 0.110)	5	0.087	(0.071 / 0.090)	33	0.075	(0.018 / 0.086)
Cu	10	0.01	(<0.01 / 0.03)	5	0.01	(<0.01 / 0.03)	33	<0.01	(<0.01 / 0.01)
Cu total	10	0.01	(<0.01 / 0.03)	5	0.02	(0.01 / 0.03)	33	0.01	(<0.01 / 0.02)
Fe	13	1.80	(0.62 / 2.80)	5	0.83	(0.24 / 1.70)	33	<0.003	(<0.003 / 0.031)
Fe^{2+}, computed[c]	13	1.07	(0.18 / 2.00)	5	0.27	(0.24 / 0.81)	33	<0.003	(<0.003 / 0.031)
Fe^{3+}, computed[c]	13	0.61	(<0.003 / 1.62)	5	0.11	(<0.003 / 1.12)	33	<0.003	(<0.003 / <0.003)
Fe, total	10	2.70	(1.40 / 3.70)	5	1.20	(0.39 / 3.00)	33	0.18	(<0.01 / 0.85)
Li	10	0.017	(0.014 / 0.026)	5	0.020	(0.016 / 0.022)	33	0.017	(0.014 / 0.026)
Mn	10	3.00	(1.80 / 4.00)	5	3.00	(1.90 / 3.70)	33	2.70	(0.55/ 3.10)
Mn, total	10	3.05	(1 70 / 4.40)	5	2.90	(1.70 / 3.70)	33	2.70	(0.57 / 3.10)
Mo	10	<0.01	(<0.01 / 0.02)	5	<0.01	(<0.01 / <0.01)	33	<0.01	(<0.01 / 0.02)
Ni	10	0.12	(0.10 / 0.15)	5	0.12	(0.12 / 0.14)	33	0.12	(0.05 / 0.15)
Ni, total	10	0.10	(0.10 / 0.20)	5	0.10	(0.10 / 0.10)	33	0.10	(<0.10 / 0.10)
Pb	10	<0.01	(<0.01 / 0.02)	5	<0.01	(<0.01 / 0.02)	33	<0.01	(<0.01 / 0.04)
Pb, total	10	<0.10	(<0.10 / 0.20)	5	<0.10	(<0.10 / 0.20)	33	<0.10	(<0.10 / 0.20)
Sr	10	0.066	(0.041 / 0.089)	5	0.068	(0.046 / 0.093)	33	0.096	(0.061 / 0.120)
V	10	<0.006	(<0.006 / <0.006)	5	<0.006	(<0.006 / <0.006)	33	<0.006	(<0.006 / <0.006)
Zn	10	0.220	(0.190 / 0.390)	5	0.230	(0.190 /0.240)	33	0.180	(0.059 / 0.370)
Zn, total	10	0.220	(0.190 / 0.390)	5	0.210	(0.200 / 0.230)	33	0.180	(0.060 / 0.370)

[a]Constituents dissolved (0.45-µm filter) and units mg L^{-1}, except as noted.[b]Water sampled at outflow from limestone drains (treated effluent) and at adjacent ditch (untreated overflow) an equivalent distance downstream from inflow.[c]Concentrations of Fe^{2+} and Fe^{3+} computed using data for Fe, Eh, and temperature-corrected equilibrium constant for the half-reaction: $Fe^{2+} = Fe^{3+} + e^-$ (as included in WATEQ4F; Ball and Nordstrom, 1991).

protozoans in suspension and in association with the hydrous Fe(III)-oxides (Robbins et al., 1997).

The OLD treatment increased pH and concentrations of Ca and alkalinity and decreased acidity of effluent relative to influent (Fig. 3, Table 1). On the basis of solute transport, effluent from each of the OLDs was statistically indistinguishable from one another, but was significantly different from the untreated AMD. Despite variations in the flow rate and chemistry of the influent during the study, the effluent from the OLDs always had pH > 6 (pH 6.2–7.0) and was net alkaline. On average, the total concentrations of solutes in the treated effluent increased by about 50% (as meq·L^{-1}) relative to the untreated influent due to added Ca and HCO_3 (Fig. 3). In contrast, AMD that bypassed the treatment and flowed about 35 m through an open ditch adjacent to the OLDs exhibited little change in chemistry relative to the upflow source (Fig. 3); the only notable changes in the untreated overflow were increased concentrations of DO and decreased total Fe, Fe^{2+} and Fe^{3+} (Table 1) due to oxidation and hydrolysis of dissolved Fe (Eqs. (2) and (3)).

As water flowed through the OLDs, concentrations of O_2, SO_4 and Mg did not change, pH and concentrations of alkalinity and Ca increased, and concentrations of acidity, Fe, and Al decreased (Table 2, Fig. 4). Despite increased pH, alkalinity, and Ca through the OLDs, limestone could dissolve throughout and neither Ca nor SO_4 could precipitate as gypsum ($CaSO_4 \cdot 2H_2O$) because the water was undersaturated with respect to calcite and gypsum (Table 2, Fig. 5a and Fig. 5b). The solute concentrations, pH, and calcite saturation index increased asymptotically, changing most rapidly near the inflow, after only a few minutes of contact with the limestone and mixing with water in the OLDs (Fig. 4 and Fig. 6). As pH increased, Fe^{3+} and Al^{3+} concentrations decreased primarily due to in situ precipitation of hydrous oxides such as amorphous $Fe(OH)_3$, ferrihydrite, schwertmannite, or goethite and amorphous $Al(OH)_3$ or poorly crystalline gibbsite (Table 2, Fig. 5c and Fig. 5d). The authors hypothesized that the hydrous oxides would not inhibit limestone dissolution but would be transported as suspended particles as water flowed rapidly (v ≥ 0.4 m/min) through the OLDs.

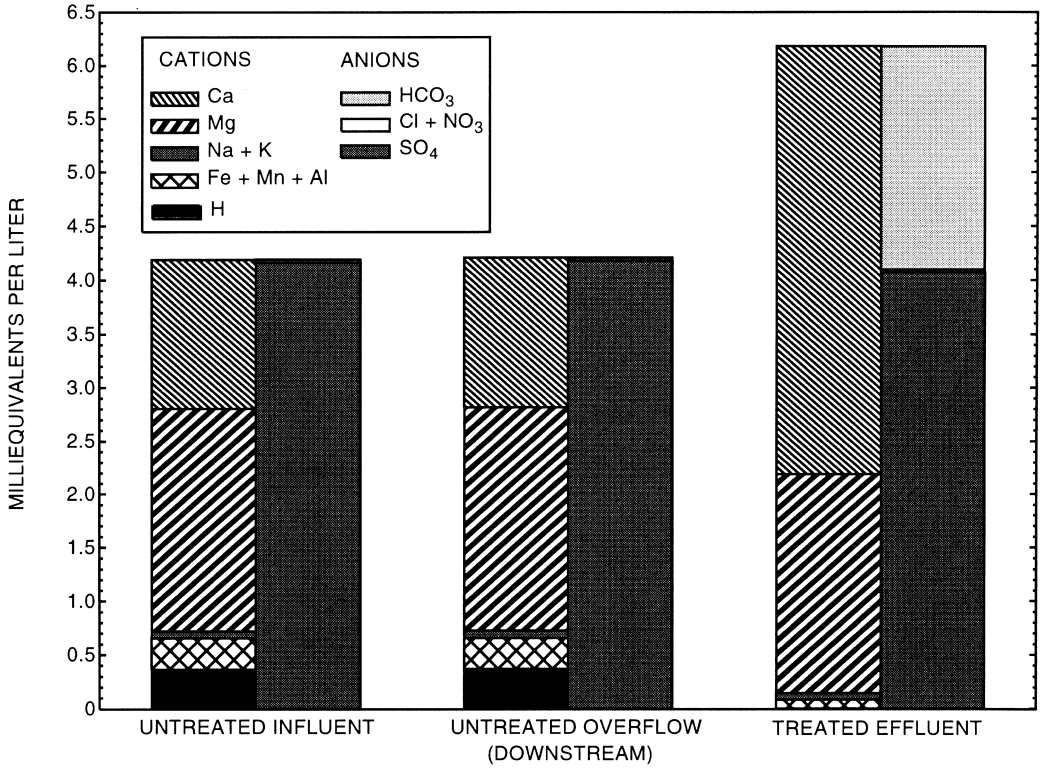

Fig. 3. Major cation and anion composition of discharge before and after treatment by OLDs. Cations and anions on left and right, respectively, stacked according to sequence shown in legend. Data are means for samples collected March 1995–March 1996 at inflow, overflow, and outflow from OLDs 1, 2, and 3.

Table 2. Measured compositions of water and calculated saturation indices at inflow and downflow within OLD-1, August 16, 1995

Parameter or constituent[a]	Distance, meters						
	0	1.5	3.0	6.1	12.2	18.3	24.4
Residence time, hours[b]	0	0.10	0.20	0.40	0.80	1.20	1.59
Specific conductance, μS/cm	430	370	380	390	420	460	620
Oxygen	2.0	1.9	1.9	1.9	1.9	1.9	2.6
Eh, volts	0.71	0.55	0.50	0.43	0.41	0.42	0.40
pH, units	3.4	4.8	4.9	5.3	6.0	6.6	6.8
Acidity, as $CaCO_3$	56	11	18	23	21	< 20	< 20
Alkalinity, as $CaCO_3$	0	8	18	26	54	84	110
SO_4	240	220	220	220	220	220	220
SiO_2	9.7	9.8	9.7	9.8	9.6	10	9.7
Ca	29	40	44	49	57	74	79
Mg	27	28	27	28	27	28	28
Na	0.9	0.9	0.9	0.9	0.9	0.9	0.9
Al	0.83	0.41	0.31	0.29	0.12	0.05	0.03
Fe	1.37	0.069	0.042	0.034	0.013	0.005	0.003
Mn	3.0	3.1	3.0	3.1	3.0	3.0	2.9
Co	0.10	0.09	0.08	0.09	0.08	0.09	0.08
Cu	0.01	< 0.01	< 0.01	< 0.01	< 0.01	< 0.01	< 0.01
Ni	0.12	0.14	0.12	0.14	0.12	0.13	0.13
Sr	0.07	0.07	0.07	0.08	0.08	0.09	0.09
Zn	0.18	0.20	0.20	0.20	0.19	0.19	0.17
Saturation index, unitless[c]							
Calcite ($CaCO_3$)	n.d.	−4.4	−3.8	−3.2	−2.1	−1.3	−0.9
Gypsum ($CaSO_4 \cdot 2H_2O$)	−1.6	−1.5	−1.5	−1.4	−1.4	−1.3	−1.3
Siderite ($FeCO_3$ ppt)	n.d.	−5.4	−5.0	−4.5	−4.0	−4.5	−4.5
Ferrihydrite [$Fe(OH)_3$]	−0.9	−0.5	−1.1	−1.2	−0.1	0.6	0.6
Goethite (FeOOH)[d]	2.6	3.0	2.4	2.3	3.4	4.1	4.1
Schwertmannite [$Fe_8O_8(OH)_6SO_4$][d]	4.2	4.6	−0.3	−1.9	5.7	9.9	9.3
$Al(OH)_3$, amorphous	−6.9	−3.2	−2.9	−1.8	−0.8	−0.4	−0.6
Gibbsite [$Al(OH)_3$]	−4.1	−0.4	−0.1	1.0	2.0	2.4	2.2
Allophane [$Al(OH)_3]_{(1-x)}(SiO_2)_x$]	−1.7	−0.7	−0.6	0.0	0.8	1.3	1.3
Jurbanite [$Al(SO_4)(OH) \cdot 5H_2O$]	−1.7	−0.7	−0.8	−0.5	−0.8	−1.6	−2.1
Basaluminite [$Al_4(SO_4)(OH)_{10} \cdot 5H_2O$]	−13.2	−1.3	−0.5	3.0	5.6	6.0	5.2
Hausmannite (Mn_3O_4)	−25.8	−20.2	−20.7	−20.0	−15.3	−10.4	−9.8
Manganite (MnOOH)	−7.2	−5.9	−6.3	−6.3	−4.7	−2.8	−2.6
Birnessite (MnO_2)	−9.6	−9.7	−10.9	−11.7	−9.8	−7.4	−7.0
Log (Pco_2, atm)[c]	n.d.	−0.8	−0.6	−0.9	−1.2	−1.6	−1.7

[a]Constituents dissolved (0.45-μm filter) and units mg L^{-1}, except as noted; n.d., no data.[b]Residence time computed as distance times cross-sectional area (0.244 m^2) times porosity (0.14) divided by volumetric flow rate. The flow rate was 0.51 m^3/hr (12.2 m^3/day) on August 16, 1995.[c]Saturation index [$SI = \log (IAP/K_T)$] and log Pco_2 calculated with WATEQ4F (Ball and Nordstrom, 1991) using tabulated data for Eh, pH, and solute concentrations plus data for K, Cl, and F; Fe and Al assumed to be at detection limit, if not detected. Temperature of the samples ranged from 11.5 to 13.3°C.[d]SI values for goethite and schwertmannite computed using activities of species calculated with WATEQ4F (Ball and Nordstrom, 1991) and solubilities reported by Bigham et al. (1996), where log $K_{GOETHITE} = 1.4$ (instead of −1.0 in WATEQ4F data base) and log $IAP_{SCHWERTMANNITE} = 18$.

During the 12-month monitoring period, the treated effluent appeared clear and contained less than 5% of the influent concentrations of acidity and dissolved Fe and Al (Fig. 7a and Fig. 7b); however, suspended particles of hydrous Fe-Al oxides and associated metals constituted a substantial proportion of the metals transport through the OLDs (Fig. 8). Initially, hydrous-oxide floc was visible only in water samples 1.5 m from the inflow ($pH \leq 5$), and dissolved Mn, Co, Ni and Zn were transported relatively conservatively through the 24.4-m long OLDs (Fig. 4b, Fig. 7b, Fig. 7c and Fig. 8); Cu was not detected in effluent. After 6 months, however, the rusty floc was visible in all samples ≤6.1 m from the inflow ($pH \leq 5.5$), and concentrations of Mn, Co, Ni and Zn in effluent declined to < 50% of influent concentrations (Fig. 4d, Fig. 7b, Fig. 7c, Fig. 8 and Fig. 9). After 9 months, the floc was present in all samples within 18.3 m of the

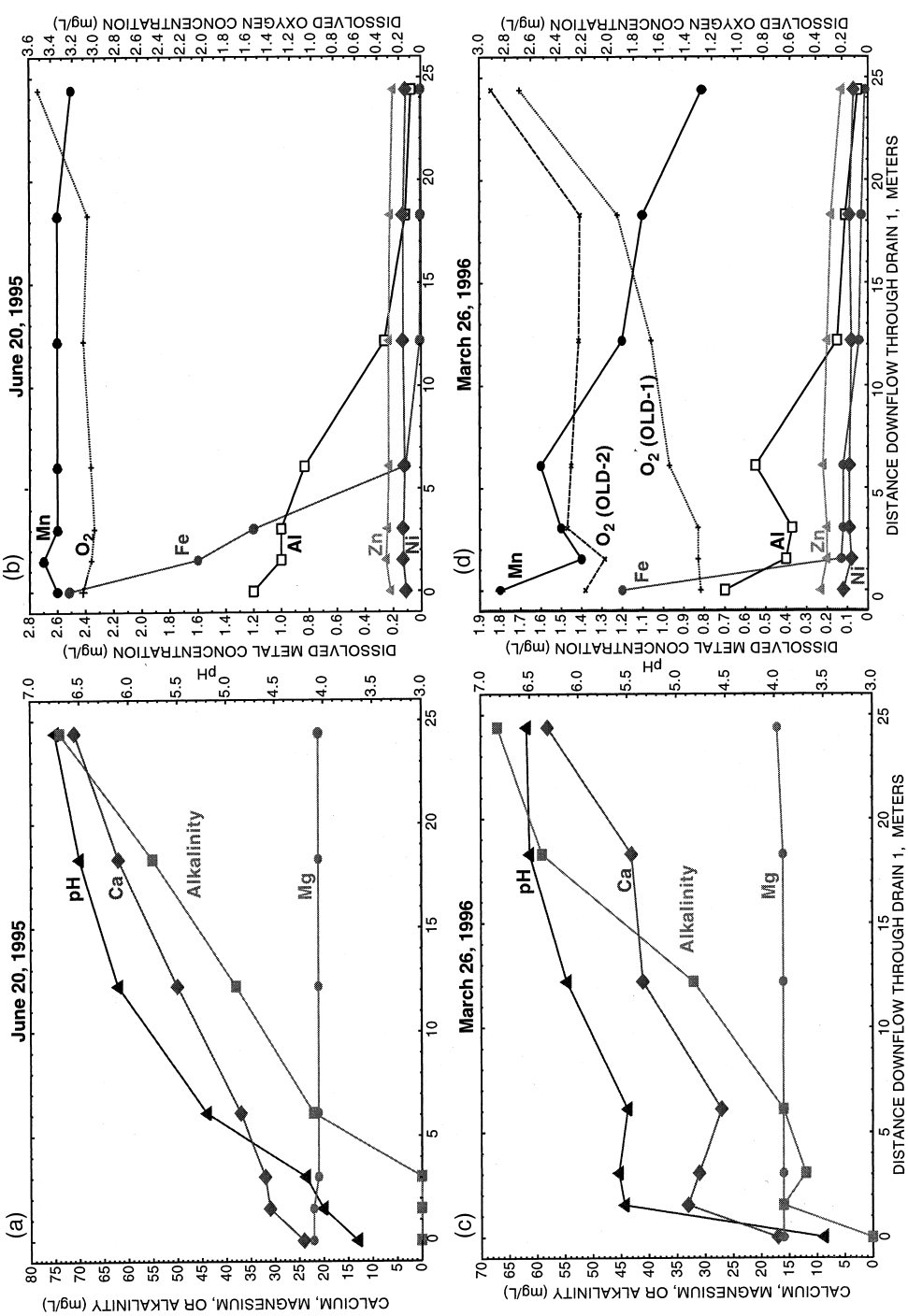

Fig. 4. Sequential changes in water chemistry within OLD-1. Data for June 20, 1995: (a) pH, and concentrations of alkalinity and dissolved Ca and Mg (b) Concentrations of dissolved O_2, Fe, Al, Mn, Zn and Ni. Data for March 26, 1996: (c) pH, and concentrations of alkalinity and dissolved Ca and Mg; and (d) Concentrations of dissolved O_2, Fe, Al, Mn, Zn and Ni. For (d), dissolved O_2 in OLD-2 (no pretreatment) is shown for comparison with OLD-1 (N_2 sparging). Samples were collected sequentially upflow; samples at 24.4 and 0 m were collected 2 and 6 hr, respectively, after starting N_2 sparging. Dissolved O_2 concentrations in effluent samples were elevated relative to upflow samples from the drains because of oxygenation within the open-ended outflow pipes; however, water-filled traps connecting the drains to the outlet pipes prevented the influx of air into the drains.

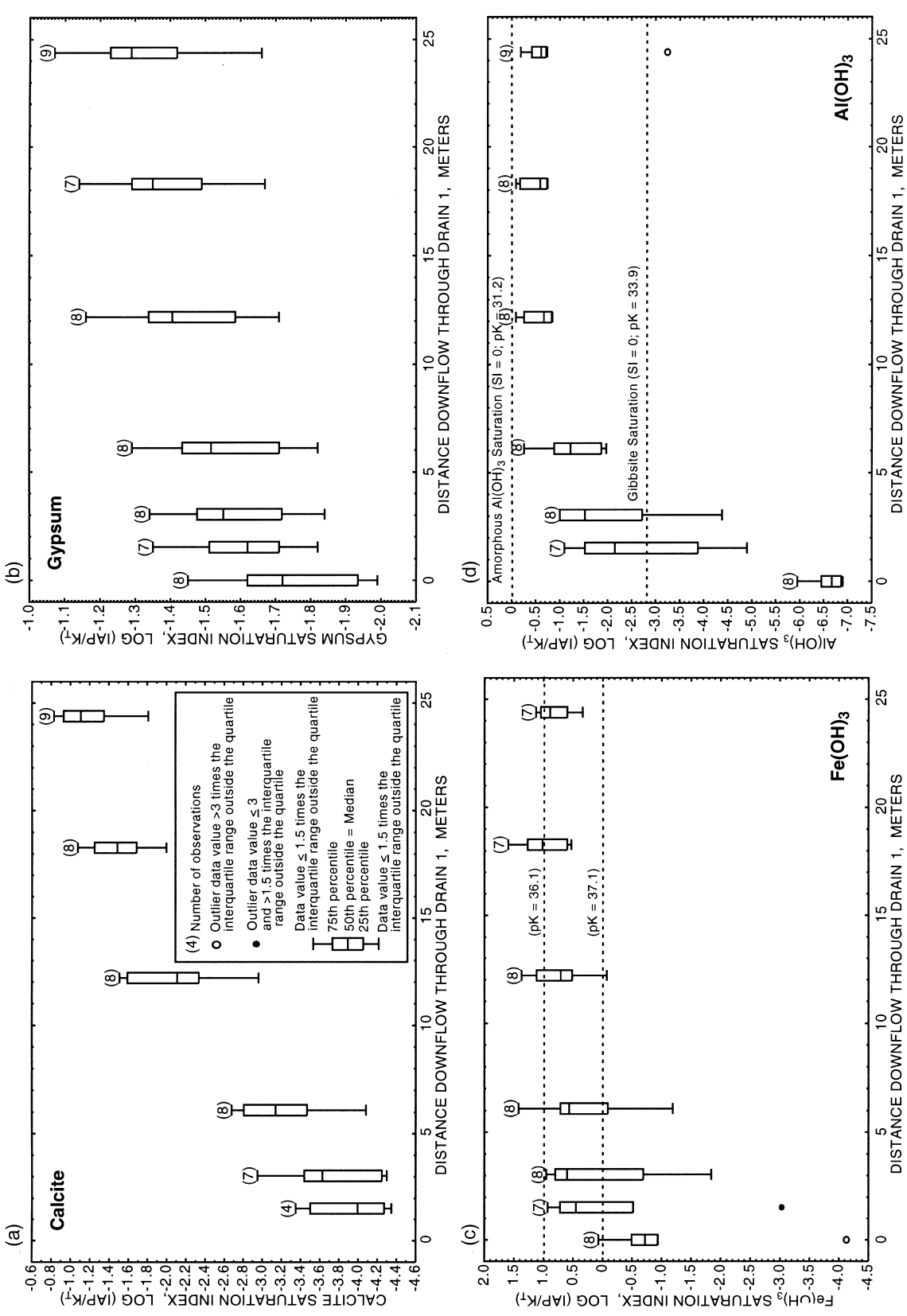

Fig. 5. Sequential changes in saturation with respect to various minerals that could dissolve or precipitate within OLD-1: (a) Calcite; (b) Gypsum; (c) $Fe(OH)_3$; and (d) $Al(OH)_3$. Saturation index calculated using the WATEQ4F computer program (Ball and Nordstrom, 1991); see notes on Table 2. Data for samples collected March 1995–March, 1996. Legend in Fig. 5a applies to entire figure.

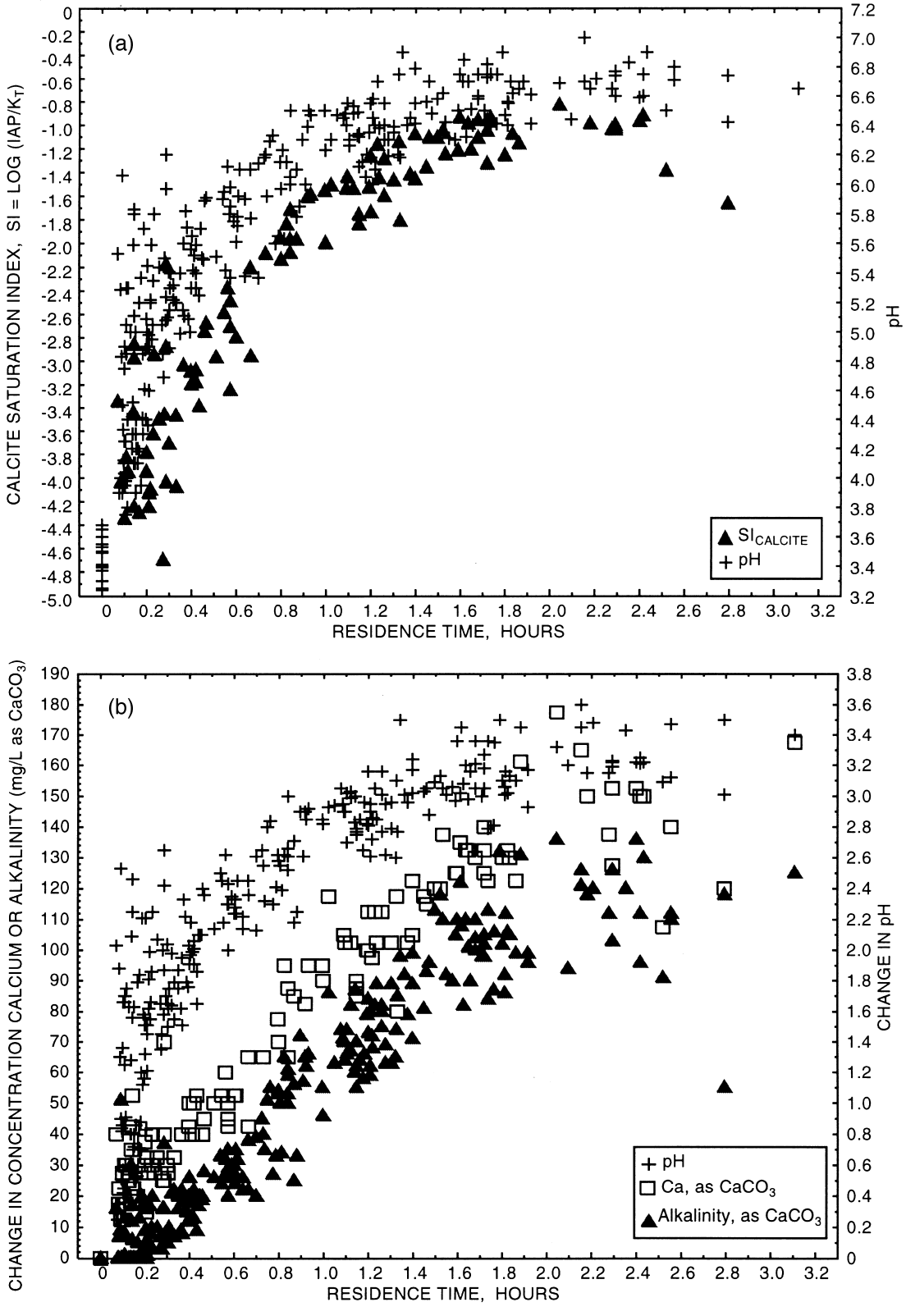

Fig. 6. Composition of water at inflow, outflow, and points within limestone drains as a function of residence time: (a) pH and calcite saturation index; and (b) Net changes in pH and concentrations of alkalinity and Ca, relative to influent composition. Data for samples collected March 1995–March, 1996 from OLDs 1, 2, and 3.

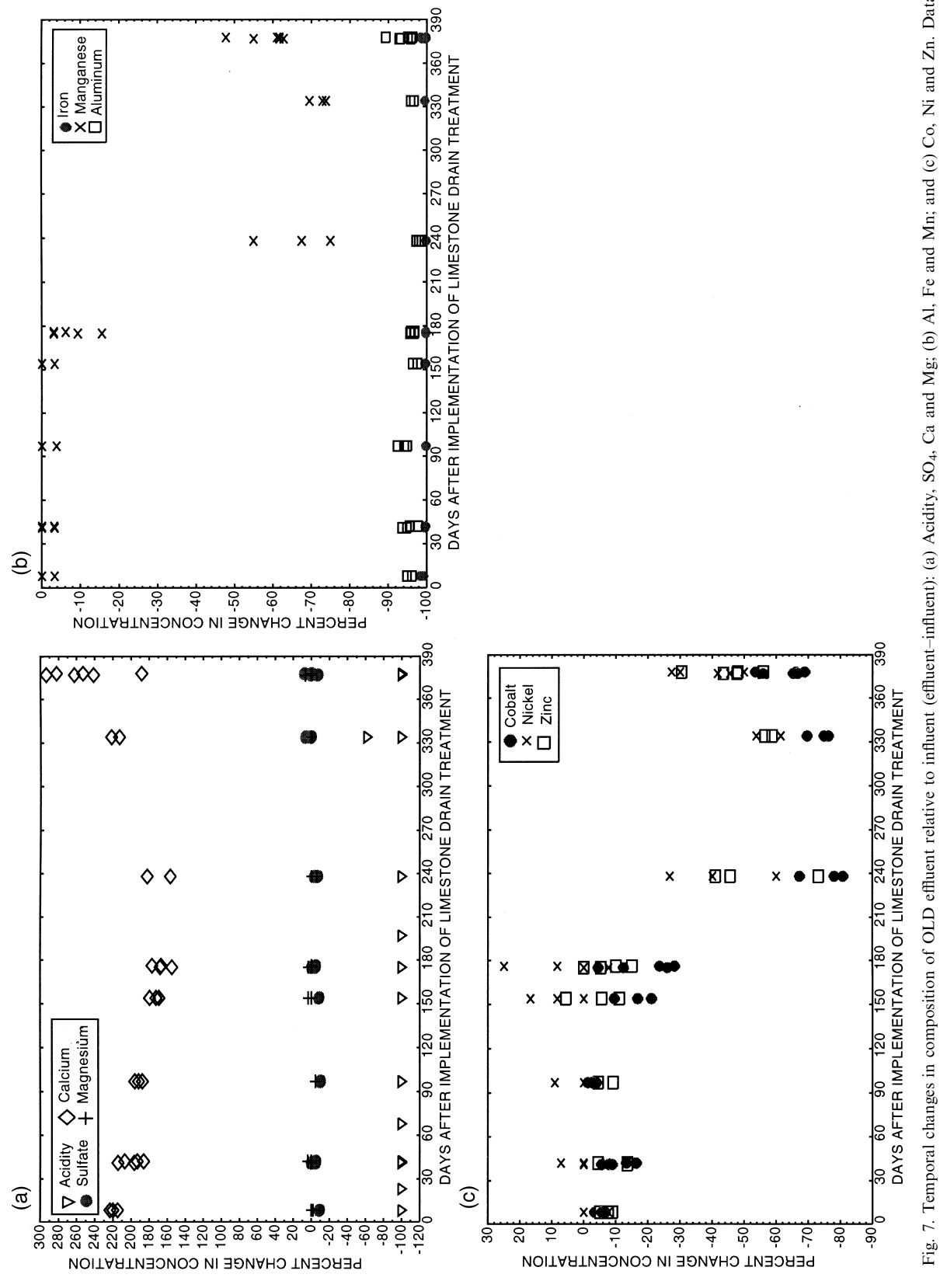

Fig. 7. Temporal changes in composition of OLD effluent relative to influent (effluent–influent): (a) Acidity, SO_4, Ca and Mg; (b) Al, Fe and Mn; and (c) Co, Ni and Zn. Data for samples collected March 1995–March, 1996 from OLDs 1, 2 and 3.

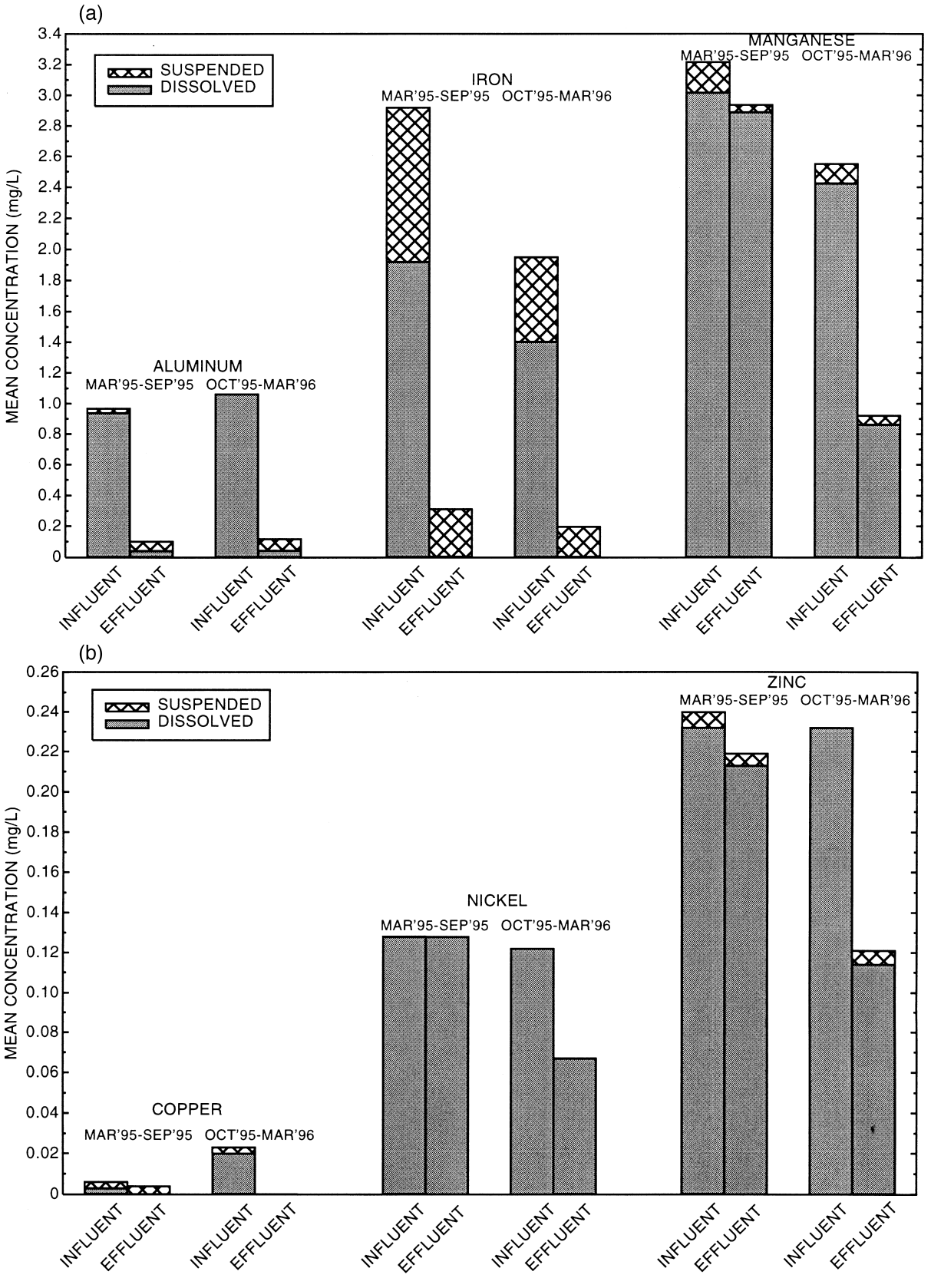

Fig. 8. Semiannual mean concentrations of suspended and dissolved metals in untreated influent and treated effluent from OLDs. (a) Al, Fe and Mn; (b) Co, Ni and Zn. Means for samples collected March 1995–September 1995 and October 1995–March 1996.

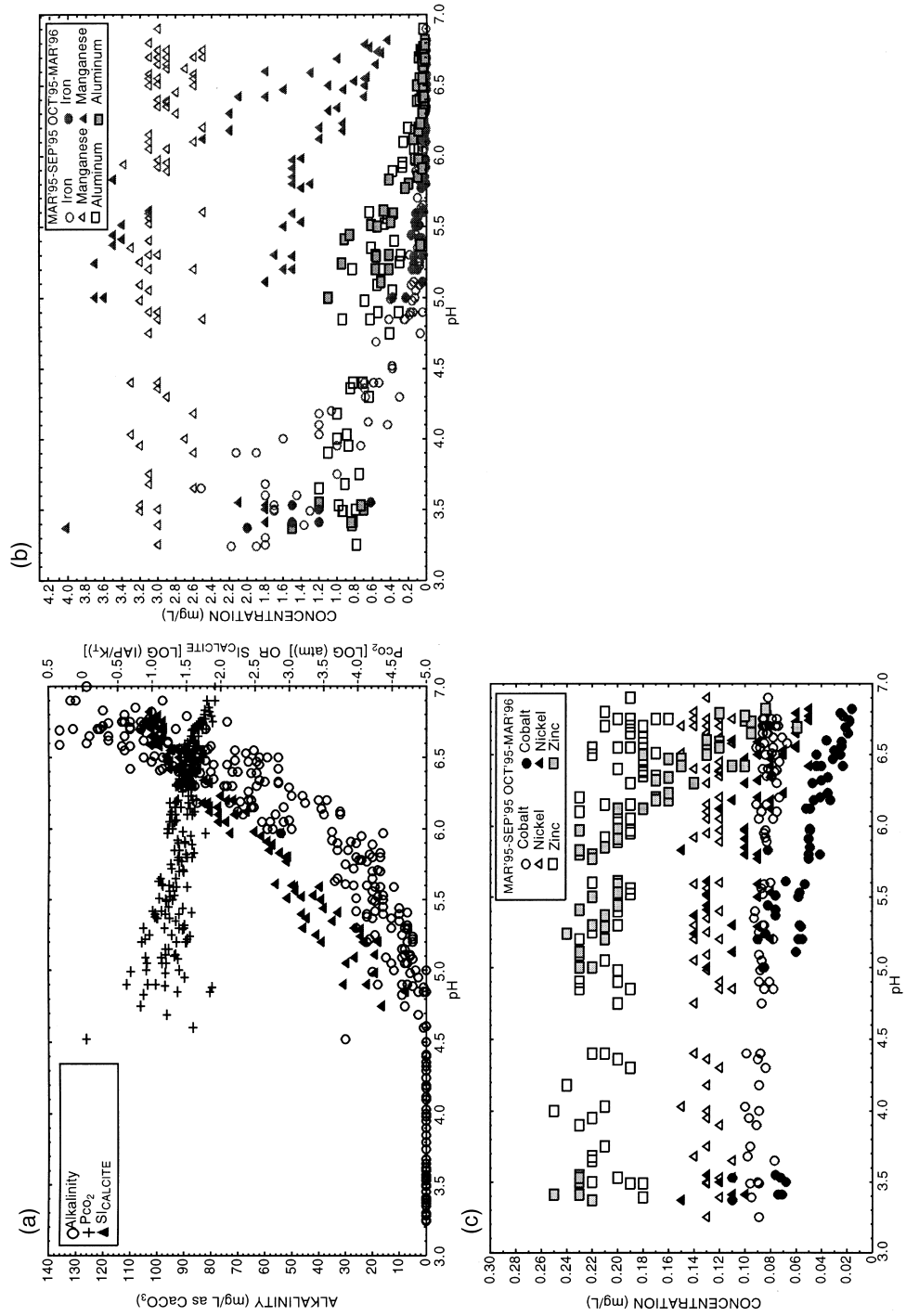

Fig. 9. Composition of water at inflow, outflow, and points within OLDs as a function of pH: (a) Alkalinity, calcite saturation index ($SI_{CALCITE}$), and partial pressure of CO_2 (Pco_2); (b) Fe, Mn and Al; and (c) Co, Ni and Zn. Data for samples collected March 1995–March, 1996 from OLDs 1, 2, and 3.

inflow ($pH \leq 7$). When monitoring ceased at 12 months, the floc had not yet appeared in the effluent; however, subsequently, the floc appeared in the effluent and could be collected from all monitoring points in the OLDs.

Downgradient trends for pH, alkalinity, Ca, Fe and Al, particularly near the inflow, became progressively more complex through time and indicated deviation from piston-flow transport implied above (compare Fig. 4a and Fig. 4b with Fig. 4c and Fig. 4d, respectively). The complex trends with respect to distance probably resulted from the localized dissolution of limestone and accumulation of hydrous oxides near the inflow that changed the porosity distribution and promoted the development of preferential flow paths. Thus, in addition to the predominant downflow transport and dispersion of hydrous oxide particles away from the inflow, turbulence could have promoted eddying and the recirculation of fluid and suspended particles locally toward the inflow. The complex trends were not an artifact of sampling where accumulated sludge could impede withdrawals of the bulk solution. Any initial turbidity in samples was depleted after only a few seconds of pumping while field-measured temperature, pH, Eh, and SC stabilized. Furthermore, pumping at ~ 1 L·min^{-1} for ≥ 10 min during routine purging and sampling would have drawn fluid from a zone ≥ 0.3 m radially from the sample intake (for porosity = 0.14). Samples drawn from only 0.2 m radially would encompass the drain cross section.

3.2. Attenuation of dissolved metals

Concentrations of Fe and Al decreased downflow through the OLDs due to the increased pH and the consequent precipitation of hydrous Fe-Al oxides (Fig. 4, Fig. 5, Fig. 7, Fig. 8 and Fig. 9). The hydrous oxides were visible as loosely bound, rust-colored coatings on limestone samples near the inflow and as a gelatinous rusty floc in water samples retrieved from the OLDs. After 2 a of operation, numerous black flakes also were visible mixed with the rusty floc. On the basis of chemistry and XRD, the solids were identified as mixtures of amorphous to crystalline Fe, Mn and Al oxides. The mixed solids were enriched in Fe (Table 3) (Fe > Al > S = Si > Mn; G. L. Nord Jr., 1998, written commun.) and contained predominantly schwertmannite and goethite (J. M. Bigham, 1997, written commun.). The black flakes were enriched in Mn (Mn > Fe = Ca > Al) and contained predominantly todorokite ($(Ca_{0.393}Mg_{0.473}Mn^{II}_{1.134})Mn^{III}_{5}O_{12}\cdot 2H_2O$) (G. L. Nord Jr., 1998, written commun.). Despite significant concentrations of Al in the solids (Table 3), the identities of crystalline Al phases could not be determined by XRD. Amorphous to poorly crystalline phases of Al, Fe, and Mn likely were present (e.g. Fig. 4c and Fig. 4d).

Table 3. Concentrations and ratios of metals encrusting limestone slabs retrieved after 5 months or 12 months immersed at inflow or within limestone drains

Sample location[a]	Weight, mg	Concentration, μg/mg								Molar ratio, mmol/mol				
		Ca	Fe	Al	Mn	Cu	Ni	Zn	Pb	Al/Fe	Mn/Fe	Cu/Fe	Ni/Fe	Zn/Fe
Samples collected August 23, 1995														
Inflow (0-m)	800.3	30	356	25	0.69	0.21	0.13	0.35	0.19	145	2.0	0.5	0.3	0.8
1–06	518.3	82	222	54	0.39	0.41	< 0.10	0.51	n.d.	503	1.8	1.6	< 0.4	2.0
2–06	311.8	192	83	32	0.23	0.23	< 0.16	0.26	n.d.	795	2.7	2.4	< 1.8	2.6
Avg. 6-m	415.1	137	153	43	0.31	0.32	< 0.13	0.38	n.d.	649	2.3	2.0	< 1.1	2.3
1–12	74.1	229	38	8.8	0.54	0.14	< 0.68	0.34	< 0.68	480	14.5	3.1	< 17.0	7.6
2–12	84.1	208	95	58	0.48	0.48	< 0.60	0.60	n.d.	1265	5.1	4.4	< 5.9	5.3
Avg. 12-m	79.1	219	67	33	0.51	0.31	< 0.64	0.47	< 0.68	872	9.8	3.8	< 11.0	6.5
Samples collected March 26, 1996														
Inflow (0-m)	361.4	n.d.	692	4	0.98	0.12	< 0.14	0.11	< 0.14	13	1.4	0.2	< 0.2	0.1
1–06	76.0	191	79	16	4.1	0.20	< 0.66	0.40	< 0.66	413	53.4	2.2	< 8.0	4.3
2–06	139.5	154	100	31	12.9	0.22	< 0.36	0.75	< 0.36	642	130.6	1.9	< 3.4	6.4
Avg. 6-m	107.8	172	90	24	8.5	0.21	< 0.51	0.58	< 0.51	528	92.0	2.0	< 5.7	5.3
1–12	78.2	256	27	10	0.96	0.13	< 0.64	0.06	< 0.64	787	36.3	4.2	< 22.6	2.0
2–12	174.4	247	40	22	2.1	0.17	< 0.29	0.26	< 0.29	1137	53.0	3.8	< 6.8	5.5
Avg. 12-m	126.3	251	33	16	1.5	0.15	< 0.46	0.16	< 0.46	962	44.6	4.0	< 14.7	3.8

[a]Sample location indicates distance, in meters, downgradient from inflow. For example, 1–06 is drain 1 at 6 m from inflow. Averages for OLD-1 and OLD-2.
n.d., not determined.

During the second 6 months of treatment (October 1995–March 1996), concentrations of dissolved Mn and trace metals declined precipitously at $pH \geq 5$ (Fig. 4d, Fig. 9b and Fig. 9c). Chemical analysis of the hydrous-oxide precipitate that coated limestone samples revealed concentrations of Mn, Cu, Ni and Zn increased relative to Fe in the coatings with distance downflow, hence with increased pH (Table 3; August 23, 1995). However, for the entire monitoring period, ratios of Mn and Zn to Fe in the coatings did not show a consistent trend with respect to pH (Table 3; March 26, 1996). The change in trace-metal content of the coatings through time probably resulted from a change in the character of the hydrous oxides at different points through the OLDs due to the variations in the accumulation of Mn with the hydrous Fe–Al oxides. Ratios of Mn/Fe and Mn/Al increased by 2 orders of magnitude during the second 6-month monitoring interval relative to the first 6 months (Table 3). Watzlaf (1997) and Brant and Ziemkiewicz (1997) also reported substantial Mn removal from AMD by limestone that had been coated by hydrous oxides after a time lag.

The removal of dissolved Mn, Zn, Ni and Co from solution (Fig. 7, Fig. 8 and Fig. 9) and the corresponding enrichment of the trace metals relative to Fe in particles and coatings on limestone (Table 3) resulted from sorption and coprecipitation reactions with the hydrous oxides of Fe(III), Mn(II-IV), and to a lesser extent Al as described by previous investigators (Hem, 1963, 1964, 1977, 1978; Loganathan and Burau, 1973; McKenzie, 1980; Benjamin and Leckie, 1981; Kooner, 1993; Coston et al., 1995; Smith et al., 1998). At the effective pH, adsorption of Mn^{2+} and trace metals on hydrous Fe and Mn oxides is very fast, on the order of minutes, and tends to be much faster than the Fe^{2+} and Mn^{2+} oxidation rates (Benjamin and Leckie, 1981; Davies and Morgan, 1989). Sorption of the trace metals generally can be enhanced by the incorporation of SO_4 with hydrous Fe(III) oxides, where the SO_4 can be part of the crystal lattice as with schwertmannite (Bigham et al., 1996; Webster et al., 1998) or can be adsorbed as with goethite or ferrihydrite (Ali and Dzombak, 1996; Rose and Ghazi, 1997). Uncoated limestone (calcite) generally is not an effective sorbent of the trace metals at $pH < 7$ (Zachara et al., 1991). Similar trends have been reported for dissolved Mn^{2+} and trace metals to adsorb to hydrous Fe, Al and Mn oxides, except that the Mn oxides are generally more effective sorbents at lower pH than Fe or Al oxides (Loganathan and Burau, 1973; McKenzie, 1980), and Zn^{2+} tends to be associated more strongly with Al oxides (Coston et al., 1995). Hence, as the Mn content of the oxides in the OLDs increased, trace-metal removal generally would be more effective at lower pH and with lower concentrations of sorbent.

Computed saturation indices indicated pure solid phases of Mn and trace metals were undersaturated throughout the OLDs (Table 2). Despite Mn-oxide undersaturation, Hem (1963) showed that when $Fe(OH)_3$ was precipitated from an aerobic, sterile solution of Mn^{2+} and Fe^{2+}, the concentration of Fe^{2+} quickly decreased, and that of Mn^{2+} also decreased although at a slower rate, so long as pH was >6.5. The autocatalytic sorption and coprecipitation reaction

$$2\,Fe(OH)_3(s) + Mn^{2+} + 2\,H^+ \longrightarrow MnO_2(s) + 4\,H_2O + 2\,Fe^{2+} \quad (11)$$

which was proposed by Hem (1964) to explain this trend, can explain the removal of Mn^{2+} and dissolved trace metals within the OLDs.[4] According to Hem (1964), Eq. (11) generally would be expected to go to the left; however, at near-neutral pH, when the activity of Fe^{2+} is very low and that of Mn^{2+} is relatively high (as found within the OLDs), the reaction will go to the right and some replacement of $Fe(OH)_3$ by MnO_2 will occur. The overall process indicated by Eq. (11) also was proposed to explain the deposition of deep-sea ferromanganese nodules composed of birnessite and todorokite, despite undersaturation of overlying waters with respect to these Mn oxides (Crerar and Barnes, 1974; Hem and Lind, 1983; Lind et al., 1987). Formation of Mn oxides within the OLDs may have been favored by near-neutral pH adjacent to limestone surfaces. At $pH \geq 6$, negatively charged surfaces of the $Fe(OH)_3$ and Mn oxides tend to attract cations, including Fe^{2+} and Mn^{2+} which can be rapidly reoxidized in an aerobic system (Tamura et al., 1976; Hem, 1977, 1978). Additionally, various other oxides can catalyze the oxidation of Mn^{2+} (Hem, 1963, 1964, 1977, 1978; Davies and Morgan, 1989, $MnO_2 > FeOOH > SiO_2 > Al_2O_3$), and microorganisms can promote the oxidation and precipitation of Mn oxides (Ehrlich, 1990; Robbins et al., 1992; Brant and Ziemkiewicz, 1997). Robbins et al. (1997) reported black Mn oxides in association with fungal hyphae and spores and with holdfasts of the "iron bacteria", *Leptothrix discophora*, that grew on

[4] Reaction 11 is an overall representation of a sequence of possible oxidation and disproportionation reactions. Naturally formed Fe–Mn oxides commonly contain MnO_2 (birnessite, pyrolusite) as a major component; however, metastable compounds of lower valent Mn, such as Mn_3O_4 (hausmannite) and MnOOH (manganite), tend to precipitate as initial products of Mn^{2+} oxidation (Hem and Lind, 1983, 1994). Subsequently, MnO_2 can form by "disproportionation" reactions whereby valence electrons in Mn_3O_4 and MnOOH spontaneously rearrange producing MnO_2 and Mn^{2+} (Bricker, 1965; Hem, 1977, 1978; Hem and Lind, 1983).

calcite suspended within the OLDs at 12.2 m (mid-flow).

3.3. Rates of iron oxidation and hydrolysis

Oxygenation of the influent was altered to evaluate potential effects of dissolved O_2 on Fe oxidation and hydrolysis and on the consequent transport or accumulation of hydrolysis products in the OLDs. During March–July 1995, influent for all 3 OLDs was pretreated by continuous N_2 sparging to decrease concentrations of dissolved O_2 entering the OLDs. During August 1995–March 1996, the continuous N_2 sparging was discontinued and, periodically, pure N_2 or O_2 gas was introduced at the inflow of OLD-1, only. However, except for variations in dissolved O_2 concentrations, no other effect resulted from the N_2 and O_2 pretreatments. The hydrochemical trends were the same for all 3 OLDs, despite periodic O_2 pretreatment of OLD-1. The effect on dissolved O_2 concentrations by N_2 sparging (OLD-1) relative to no pretreatment (OLD-2) is shown in Fig. 4d. At the most vigorous N_2 sparging rate, less than half of the dissolved O_2 in the influent was removed ($2.0\ mg{\cdot}L^{-1} = 10^{-4.20}\ mol{\cdot}L^{-1}$ decreased to $1.3\ mg{\cdot}L^{-1} = 10^{-4.39}\ mol{\cdot}L^{-1}$). Nevertheless, because only 0.25 mol of O_2 is needed to oxidize 1 mol of Fe^{2+} (Eq. (2)), even the minimum measured concentration of dissolved O_2 in the N_2-sparged or raw discharge water ($10^{-4.45}\ mol{\cdot}L^{-1} = 0.93\ mg{\cdot}L^{-1}$) was more than 4 times the amount required to oxidize the maximum Fe^{2+} ($10^{-4.45}\ mol{\cdot}L^{-1} = 2.0\ mg{\cdot}L^{-1}$) in the influent. Furthermore, residence times of 1–3 hr for water in the OLDs (Fig. 2 and Fig. 6) generally were sufficient for nearly complete oxidation of Fe^{2+} in the OLDs.

Total dissolved Fe was attenuated at pH <6 (Fig. 4 and 9b) due to oxidation and hydrolysis within the OLDs. Williamson et al. (1992) indicated that the biological oxidation rate for Fe^{2+} in surface waters receiving AMD is both faster than the abiotic oxidation rate and independent of pH over the range 2.5 to 6.0, as indicated by the differential rate expression:

$$d - [Fe^{2+}]/dt = k[Fe^{2+}], \quad (12)$$

where $k = 10^{-3.61}\ s^{-1}$ and $[Fe^{2+}]$ denotes concentration (in $mol{\cdot}L^{-1}$). After integration of Eq. (12), the concentration of residual Fe^{2+} can be computed for elapsed time, t (in seconds):

$$[Fe]_t = [Fe]_{t=0}\exp\{-k \cdot t\} \quad (13)$$

Thus, for a maximum initial concentration of Fe^{2+} of $2\ mg{\cdot}L^{-1}$ and for residence times of 3 hr and 1 hr, Eq. (13) indicates the amount of Fe^{2+} remaining in solution would be $0.141\ mg{\cdot}L^{-1}$ and $0.827\ mg{\cdot}L^{-1}$, respectively. Thus, 7 to 40% of the initial concentrations of Fe^{2+} would be expected in the effluent from the OLDs, with an increasing percentage for decreasing residence time. Because any Fe^{3+} in the influent or produced by in situ oxidation of Fe^{2+} would rapidly precipitate as $Fe(OH)_3$ or related compounds, total dissolved Fe in effluent would be expected to decrease by a greater percentage than that for Fe^{2+}. The computed concentrations of Fe^{2+} compare favorably with Fe^{2+} data for the untreated bypassed flow (Table 1); however, the computed values are several orders of magnitude higher than concentrations of Fe^{2+} or Fe measured in the effluent from the OLDs ($Fe \leq 0.003\ mg{\cdot}L^{-1}$, Table 1). The measured rates of Fe removal also exceed Fe^{2+} oxidation rates for AMD in a continuously-stirred tank reactor at other field sites and considering variations in the biotic and abiotic Fe^{2+} oxidation rate as a function of pH (Kirby and Elder Brady, 1998; C. S. Kirby, 1997, written commun.). Additional processes such as sorption could account for the extensive removal of dissolved Fe^{2+} by the OLDs. Retention time and Fe^{2+} oxidation can be increased by sorption of Fe^{2+} and catalysis of oxidation by $Fe(OH)_3$ at near-neutral pH (Tamura et al., 1976; Stumm and Sulzberger, 1992).

3.4. Rates of limestone dissolution

Limestone would tend to dissolve throughout the OLDs because the water was undersaturated with respect to calcite under the conditions evaluated (Fig. 5a, Fig. 6a and Fig. 9a). However, limestone dissolution was more extensive near the inflow where the water was farthest from saturation (most aggressive). The rate of limestone dissolution is expected to decline as conditions within the drain approach calcite saturation. The calcite saturation index ($SI_{CALCITE}$) increased asymptotically with distance (Fig. 5a) or residence time (Fig. 6a) and linearly with pH (Fig. 9a). After 1 hr residence time, the water in the OLDs was net alkaline and had pH $\sim$6 and $SI_{CALCITE} - 2$; however, by tripling residence time from 1 to 3 hr, pH increased only to $\sim$6.8 while $SI_{CALCITE}$ increased to -1 (Fig. 6a) and alkalinity and Ca concentrations doubled from about 60 to 120 $mg{\cdot}L^{-1}$ and 90 to 180 $mg{\cdot}L^{-1}$, respectively (Fig. 6b and Fig. 10a).[5]

Limestone and calcite samples, which were suspended at the inflow and at downflow points within the drains, showed effects of both precipitation and dissolution, particularly near the inflow. Microscopic examination of calcite mounts on glass slides showed

[5] Because alkalinity could not be measured for pH <4.5, the concentration of dissolved Ca is a better indicator of limestone dissolution.

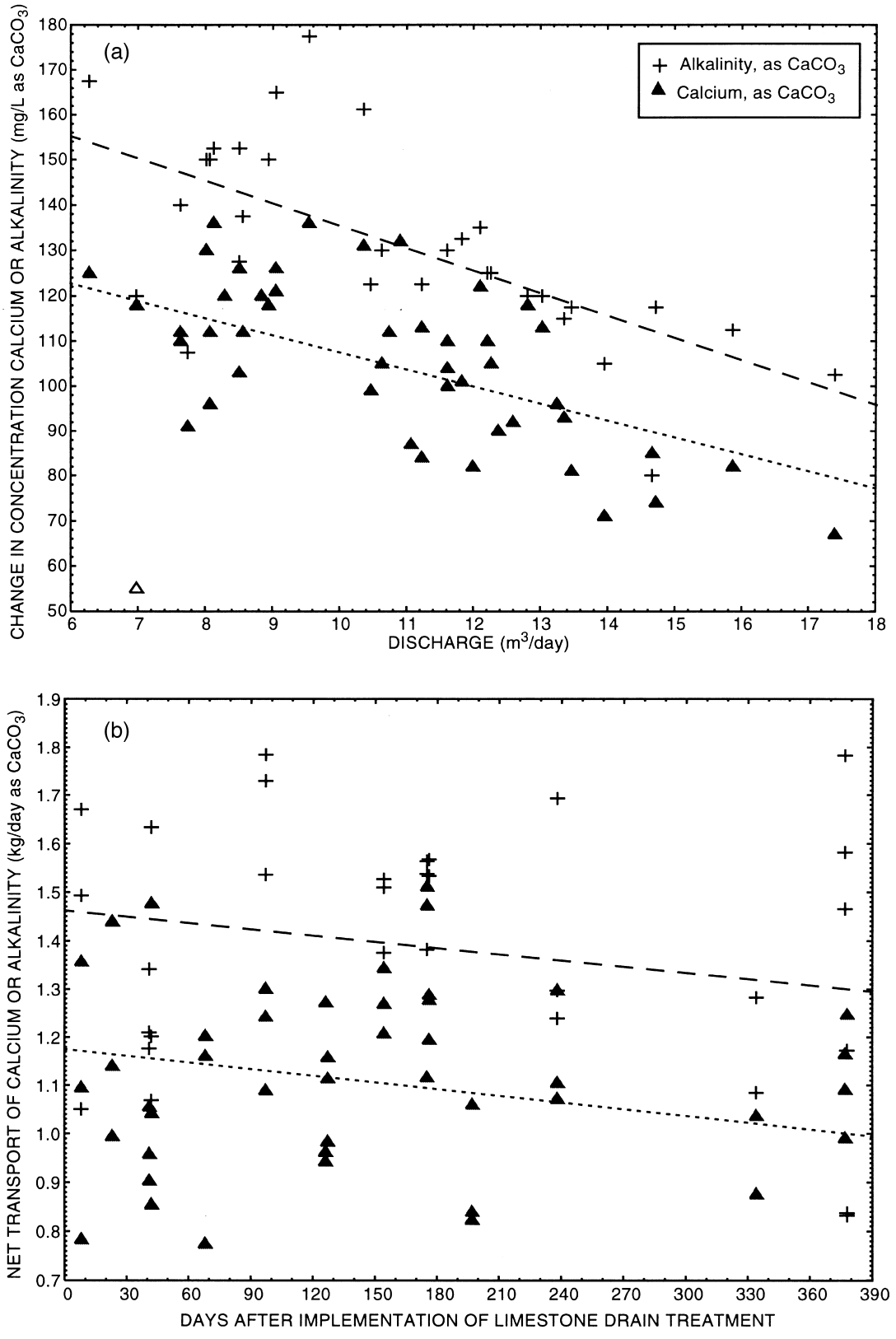

Fig. 10. Amount of Ca and alkalinity added to effluent from OLDs: (a) Concentrations as a function of discharge rate; (b) Transport as a function of elapsed time since initial use of the drains. Data for samples collected March 1995–March, 1996 from OLDs 1, 2, and 3. Dashed and dotted regression lines indicated for Ca and alkalinity, respectively. Slopes of regression lines are highly significant with respect to discharge rate ($r > 0.51$; $P < 0.01$) but insignificant with respect to elapsed time ($r < 0.24$; $P > 0.10$).

newly formed Fe and Mn oxide and dissolution etch pits (Robbins et al., 1997). After rinsing off the hydrous oxide crusts, initially dark gray, smooth-surfaced limestone slabs appeared powdery white and grainy, and initially colorless calcite rhombs were stained orange. Although accumulations of the hydrous oxides on limestone were relatively thick (~1 mm) at the inflow to the drains, $CaCO_3$ dissolution rates remained

Table 4. Rates of limestone dissolution computed on the basis of calcite and limestone retrieved after 5 months or 12 months immersed at inflow or within limestone drains

Sample location[a]	Surface area, cm^2	Initial weight, g	Final weight, g	Weight loss, %	Dissolution rate[b]	
					$g \cdot g^{-1} \cdot a^{-1}$	$\log(mmol \cdot cm^{-2} \cdot s^{-1})$
Calcite rhombs immersed within limestone drain for 5 months (March 23, 1995–August 23, 1995)						
1–06	44.98	51.7894	50.1873	3.093	0.0737	−7.57
2–06	33.76	33.5450	32.6167	2.767	0.0660	−7.68
Avg. 6-m						−7.63
1–12	41.08	42.4943	41.5750	2.163	0.0516	−7.77
2–12	44.82	52.7958	51.7851	1.914	0.0456	−7.77
Avg. 12–m						−7.77
Limestone slabs immersed within limestone drain for 5 months (March 23, 1995–August 23, 1995)						
Inflow	42.12	43.3788	34.0796	21.43	0.5114	−6.78
Inflow	44.10	49.9887	40.9369	18.10	0.4319	−6.81
Inflow	35.52	31.5680	26.9189	14.72	0.3513	−7.00
Avg. 0-m						−6.86
1–06	41.80	46.0653	43.8176	4.879	0.1164	−7.39
1–06	42.30	47.6974	45.1482	5.344	0.1275	−7.34
1–06	20.06	17.4558	16.0444	8.085	0.1928	−7.27
2–06	34.98	30.3221	28.5925	5.704	0.1360	−7.43
2–06	28.18	27.0120	25.6713	4.963	0.1184	−7.44
2–06	35.92	33.7302	31.9752	5.203	0.1241	−7.43
Avg. 6-m						−7.39
1–12	39.08	34.9815	33.6858	3.703	0.0883	−7.60
1–12	43.34	49.6653	48.0459	3.260	0.0777	−7.55
1–12	39.42	46.3258	44.4346	4.082	0.0973	−7.44
2–12	35.52	32.2868	31.4310	2.650	0.0632	−7.74
2–12	35.02	32.2045	31.1104	3.397	0.0810	−7.63
2–12	33.32	32.8591	31.8046	3.209	0.0765	−7.62
Avg. 12-m						−7.60
Limestone slabs immersed within limestone drain or 12 months (March 23, 1995–March 26, 1996)						
1–06	38.56	40.0301	37.2362	6.979	0.0692	−7.64
1–06	35.50	37.2105	35.5586	4.439	0.0440	−7.83
1–06	36.94	35.0955	33.2948	5.130	0.0508	−7.81
2–06	39.68	30.8110	27.8474	9.618	0.0954	−7.63
2–06	34.4	30.9177	28.7229	7.098	0.0704	−7.70
2–06	30.16	36.9740	35.5580	3.829	0.0379	−7.83
Avg. 6–m						−7.74
1–12	41.16	36.9858	35.2625	4.659	0.0462	−7.88
1–12	33.06	32.9569	31.8929	3.228	0.0320	−7.99
1–12	20.46	23.1696	22.3484	3.544	0.0351	−7.90
2–12	26.72	22.4805	20.8161	7.403	0.0734	−7.71
2–12	27.02	25.4095	24.2530	4.551	0.0451	−7.87
2–12	32.44	29.0688	28.0004	3.675	0.0364	−7.99
Avg. 12-m						−7.89

[a]Samples had been immersed continuously at fixed locations at inflow or within a specific limestone drain. Sample location indicates OLD-1 or 2 and distance, in meters, downgradient from inflow (at 0 m). For example, 1–06 is drain 1 at 6 m from inflow. Averages for OLD-1 and OLD-2.

[b]Dissolution rate computed using initial mass and surface area of samples; no adjustment made for expected decreases in these parameters through time. Rates normalized using specific surface area (A_{SP}); mean $A_{SP} = 0.884$ and 1.004 $cm^2 \cdot g^{-1}$ for 19 calcite rhombs and 75 limestone slabs, respectively.

greater at the inflow than at downflow points within the drain where such accumulations were thin to non-existent (Table 4). The correlation between $CaCO_3$-dissolution rate and amount of encrustation (Table 3 and Table 4) results because the dissolution and precipitation processes are most extensive under initial conditions of low pH and high Fe^{3+} concentrations, respectively (Table 1 and Table 2). The calculated $CaCO_3$ dissolution rates decreased with increased pH and activities of Ca^{2+} and HCO_3^- and decreased Pco_2. During the initial 6 months, the limestone dissolution rate was $10^{-6.9}$ mmol·cm^{-1}·s^{-1} at the inflow (pH = 3.5–4) and $10^{-7.6}$ mmol·cm^{-2}·s^{-1} at the midflow (pH = 6–6.5); the dissolution rates for calcite rhombs were slightly less than those for limestone slabs subjected to identical conditions (Table 4). These trends are consistent with rate laws established by laboratory experiments which used HCl to maintain constant pH as rotating calcite discs dissolved (Plummer et al., 1979; Arakaki and Mucci, 1995). However, the field rates for $CaCO_3$ reaction with AMD (Table 4) are about an order of magnitude less than the reported laboratory rates at comparable pH. In a recent evaluation, Aschenbach (1995) demonstrated that calcite dissolved more rapidly in HCl solutions than in synthetic AMD (H_2SO_4 solutions) for a given pH and that calcite remained indefinitely undersaturated in the synthetic AMD at near-neutral pH. A similar trend of calcite undersaturation in the OLDs is indicated by the asymptotic, marginal increase in $SI_{CALCITE}$ with residence time (Fig. 6a).

The concentrations of Ca and alkalinity added to treated effluent were greatest for slowest flow rates or longest residence time (Fig. 6b and Fig. 10a). However, the overall limestone dissolution rate, as indicated by the daily transport of Ca and alkalinity, was independent of flow rate and did not change significantly during the study period (Fig. 7a and Fig. 10b). The cumulative limestone dissolution rate for the 3 OLDs combined was 4.4 kg·d^{-1} on the basis of net Ca transport. This dissolution rate of 4.4 kg·d^{-1} (Q = 29.9 m^3·d^{-1}; t_R = 2 hr) is equivalent to a dissolution rate of 0.042 g·g^{-1}·a^{-1} or $10^{-7.9}$ mmol·cm^{-2}·s^{-1} computed for limestone samples immersed for 1 a at the 12.2-m midpoint of OLD-1 (Table 4)[6] and is intermediate to rates of 17.9 and 2.7 kg·d^{-1} for the Howe Bridge (Q = 138 m^3·d^{-1}; t_R = 23 hr) and Morrison (Q = 9.8 m^3·d^{-1}; t_R = 51 hr) ALDs, respectively (Hedin et al., 1994b). On the basis of the limestone dissolution rate of 4.4 kg·d^{-1} and the total of 38 200 kg of limestone, linear extrapolation indicates that the limestone used to build the OLDs could theoretically last 24 a.

3.5. Design considerations for limestone drains

The residence time for water in the limestone drains is a critical factor affecting their performance because of kinetic controls on dissolution, precipitation, and sorption reactions that control pH and dissolved ion concentrations. Thus, Hedin and Watzlaf (1994) evaluated construction characteristics, residence times, and chemistry of influent and effluent of more than 20 limestone drains to determine the optimum size for maximum alkalinity production. They derived the following sizing technique, which was incorporated into guidelines of Hedin et al. (1994a):

$$M_S = Q \cdot ((t_L \cdot C/x) + (t_R \cdot \rho_b/n)) \quad (14)$$

Eq. (14) computes the mass of limestone, M_S, needed for treatment of AMD of a given flow rate, Q. Variables in the first term include the desired longevity of treatment (t_L), desired alkalinity concentration for the effluent (C), and the purity of limestone expressed as $CaCO_3$ mole fraction (x). Additional variables in the second term assure a specified residence time to achieve the maximum alkalinity and are the same as those for Eq. (10). In this study, measured values for $t_R \leq 3.1$ hr; $\rho_b = 2140$ kg·m^{-3}; and n = 0.14 indicate that values assumed by Hedin and coworkers for t_R = 15 hr; $\rho_b = 1600$ kg·m^{-3}; and n = 0.5 could be poor estimates for the second term, particularly for drains that used tabular, mixed-size limestone fragments. The 5-fold difference in estimated residence time does not cause a problem, however, because errors in the term specifying residence time cancel due to the interdependence of t_R, ρ_b and n. For example, computed mass of limestone required for a given flow rate is the same using consistent data from Hedin and coworkers or this study, where $(t_R \cdot \rho_b/n) = (15 \cdot 1600/0.5) = (3.1 \cdot 2140/0.14)$, respectively. Nevertheless, the dimensions of the area or trench for installaiton would be affected by the assumed value for bulk density, because the same mass of limestone would occupy one-third larger volume for $\rho_b = 1600$ kg·m^{-3} than for $\rho_b = 2140$ kg·m^{-3}. Furthermore, rate-dependent reactions and potential for abrasion and transport of hydrous oxides from the drains can be misunderstood if residence time and velocity of flow are poorly characterized.

Hedin et al. (1994a) advised against the use of horizontally oriented limestone drains for treatment of AMD containing >1 mg·L^{-1} of O_2, Fe^{3+} or Al^{3+}

[6] A dissolution rate of 0.042 g·g^{-1}·a^{-1} = 4.4 kg·d^{-1}·365 d·a^{-1}/38 200 kg. Using the average specific surface area for limestone slabs, the dissolution rate can be normalized to $10^{-7.9}$ mmol·cm^{-2}·s^{-1} = 0.042 g·g^{-1}·a^{-1}·1.004 g·cm^{-2}/(0.1 g·mmol^{-1}·107.5 s·a^{-1}).

due to potential for armoring and clogging of the drains. However, results of this study combined with recent results of Watzlaf (1997), Sterner et al. (1998), and Brant and Ziemkiewicz (1997) suggest that limestone treatment systems can effectively increase pH and remove dissolved metals, including Mn^{2+}, from AMD containing moderate concentrations of O_2, Fe^{3+} or Al^{3+} (1–5 mg·L^{-1}).

In an OLD, oxidation and hydrolysis reactions will proceed and the solid and dissolved products will accumulate to some extent within the treatment system. Dissolved H^+ and CO_2 in the untreated AMD and generated as hydrolysis products within an OLD (Eqs. (3) and (7)) will react with the limestone (Eqs. (4) and (5)). The following overall reaction, which combines Eqs. (2), (3), (4), (5) and (7), shows alkalinity as an ultimate product of the Fe hydrolysis reaction in an OLD:

$$Fe^{2+} + 0.25\,O_2 + 2\,CaCO_3 + 2.5\,H_2O \longrightarrow Fe(OH)_3 + 2\,Ca^{2+} + 2\,HCO_3^- \quad (15)$$

where 2 moles of $CaCO_3$ dissolve for each mole of $Fe(OH)_3$ produced. Hence, in an OLD, rapidly dissolving limestone surfaces may not be stable substrates for $Fe(OH)_3$ attachment and armoring. Because overall efficiency can be increased by combining neutralization and hydrolysis reactions, an OLD may require less land area than needed to construct an ALD and subsequent oxidation pond. Limestone near the inflow to the drains that was loosely coated by $Fe(OH)_3$ dissolved more rapidly than uncoated limestone that was downflow. The measured flow velocities of 0.1 to 0.4 m·m^{-1} associated with residence times of ≤3.1 hr were adequate to transport a fraction of the solid hydrolysis products ($Fe(OH)_3$, $Al(OH)_3$, MnO_2) through the drains as suspended particles. As demonstrated by this study, trace metals can be removed from solution by sorption and coprecipitation with the hydrous Fe, Mn, and Al oxides within the drains. However, insufficient time elapsed during the study to evaluate the potential for steady-state formation and transport of the hydrolysis products whereby total concentrations of metals (dissolved + suspended solids) in influent and effluent are equal. Furthermore, because the redox state of Fe could not be effectively controlled in the field experiment as conducted, rates of dissolution, precipitation, and sorption reactions over a range of redox conditions at constant pH could not be evaluated. Comparable data on limestone dissolution rates and metal attenuation rates have not been reported for other limestone drains or for more mineralized AMD.

Elongate structures, such as the drains used for the subject experiments, or narrow meandering structures could provide sufficient residence times and high flow velocities necessary to achieve neutralization of AMD and transport of hydrolysis products. If the water contains Fe^{2+} and Mn^{2+}, hydrolysis reactions can be promoted by introducing O_2. To enhance trace-metal attenuation by hydrous oxide particles within the drains, the cross-section of the drain could be enlarged near the outflow to decrease flow velocities and increase residence time where pH is expected to be highest. To insure against clogging from an excessive accumulation of hydrous oxides, perforated piping could be installed as subdrains for periodic flushing of excess sludge. Some of these conceptual designs have recently been constructed but have not been evaluated (C. A. Cravotta, 1997, unpublished data; G. R. Watzlaf, 1997, oral commun.). Additional studies are needed to evaluate such designs and to determine optimum criteria for utilization and construction of limestone drains for AMD remediation. In general, additional information is needed to understand potential for, and effects of, the dissolution of limestone and the formation, accumulation and transport of secondary metal compounds in AMD treatment systems. Because of the wide range of water-chemistry and hydrologic conditions at coal and metal mines (Rose and Cravotta, 1998; Nordstrom and Alpers, 1998), simple to complex remedial alternatives could be appropriate depending on site characteristics.

4. Conclusions

This study showed that enclosed limestone drains can be effective for neutralizing oxic, relatively dilute AMD ($O_2 > 1$ mg·L^{-1}; acidity < 90 mg·L^{-1}) and decreasing concentrations of dissolved Al^{3+}, Fe^{3+}, Fe^{2+}, Mn^{3+} and trace metals (< 5 mg·L^{-1}). In less than 3 hr residence time, limestone dissolution within the drains increased pH from 3.5 to ≥6.2, producing net alkaline effluent. The effluent was undersaturated with respect to calcite. With increased distance, downflow through the drains, and accordingly with increased residence time for a given flow rate, the following trends were observed: (1) pH and concentrations of alkalinity and Ca increased; (2) acidity, Fe and Al decreased, ultimately to $< 5\%$ of influent concentrations; and (3) O_2, SO_4 and Mg did not change. After flowing a short distance through the drains, the water became saturated with hydrous Fe and Al oxides which formed loosely bound, orange-yellow coatings on limestone near the inflow and suspended particles at sampling points downflow. Low concentrations of dissolved O_2 throughout the drains exceeded that needed (< 0.3 mg·L^{-1}) for the oxidation of all Fe^{2+} (< 2 mg·L^{-1}) in the influent; however, nearly complete removal of dissolved Fe greatly exceeded the expected rate of removal by coupled Fe^{2+} oxidation and Fe^{3+}

hydrolysis, indicating that sorption and coprecipitation of Fe^{2+}, Fe^{3+} and other cations could be important.

The accumulated hydrous oxides and elevated pH (>5) within the OLDs promoted sorption and coprecipitation of Fe^{2+}, Mn^{2+}, Pb^{2+}, Cu^{2+}, Co^{2+}, Ni^{2+} and Zn^{2+} with the hydrous oxides. Although undersaturated with Mn, Co, Ni, and Zn compounds, concentrations of dissolved metals in the effluent decreased by ≥50% relative to the influent after hydrous oxides had accumulated in downflow parts of the drains. With increased distance downflow, hence with increased pH, concentrations of Mn, Cu, Co, Ni and Zn in the water decreased while those in the corresponding hydrous oxides increased relative to Fe. The removal of dissolved Mn^{2+}, by the autocatalytic reaction of Mn^{2+} with $Fe(OH)_3$, also produced Mn oxides. The hydrous Fe, Mn and Al oxides are effective sorbents and catalysts for oxidation of Fe^{2+} and Mn^{2+} at near-neutral pH. Consequently, at pH >5 within the OLDs, negatively charged surfaces of the oxides could attract and attenuate Fe^{2+}, Mn^{2+}, Pb^{2+}, Cu^{2+}, Co^{2+}, Ni^{2+} and Zn^{2+}. Extensive oxidation of Fe^{2+} and Mn^{2+} was possible due to attenuation and catalysis by the oxides. Microorganisms associated with the oxides also could have catalyzed the oxidation and attenuation of Fe^{2+}, Mn^{2+} and other metals.

The rate of limestone dissolution was minimally affected by the accumulation of hydrous Fe–Mn–Al oxides as loosely bound coatings. Despite the ~1-mm thick accumulation of hydrous oxides on limestone surfaces, pH increased most rapidly near the inflow as a result aggressive dissolution of limestone by the influent AMD. The rate of limestone dissolution decreased with increased pH and concentrations of Ca^{2+} and HCO_3^- and decreased Pco_3. Under the "closed system" conditions in which hydrolysis products including H^+ and CO_2 could not escape the drains and were retained as reactants, limestone surfaces rapidly dissolved, and true armoring was avoided, despite oxygenated conditions. However, the computed dissolution rates for the field experiment were about an order of magnitude less than reported laboratory rates at comparable pH. The reason for slower rates of $CaCO_3$ dissolution by AMD (field) than by HCl (laboratory) was not determined but could involve variations in ion pairing, surface charge, and potential for various minerals to precipitate on the surface. Additional studies are needed to determine the hydrochemical conditions and role of microorganisms in mineral precipitation reactions that promote or inhibit limestone dissolution and ultimately can cause failure of limestone treatment systems.

Although only a small fraction of the solid hydrolysis products was transported through the OLDs during the study, the progressive accumulation of hydrous oxides at increased distances downflow indicated eventual breakthrough of particle-rich effluent was probable. In fact, samples collected in 1997 verify the breakthrough of suspended particles, which cause the effluent to be turbid. Monitoring generally would be needed for extended periods to evaluate the potential for steady-state formation and transport of hydrolysis products and the ultimate longevity of treatment on and systems. Different conceptual designs may be considered for promoting the transport of hydrous oxides and optimizing the long-term neutralization of AMD and removal of dissolved metals. Before criteria can be refined for the construction of OLDs to neutralize AMD, however, various innovative conceptual designs need to be tested, and available data for existing systems need to be evaluated. Accurate information on variations in the water chemistry, residence time, rates of limestone dissolution, and effects of hydrolysis products on limestone dissolution, sorption of trace metals, and hydraulic properties is needed to optimize designs for OLDs and ALDs and to minimize costs for effective implementation of these passive-treatment systems.

Acknowledgements

This study was conducted by the USGS in cooperation with the Pennsylvania Department of Environmental Protection. R.C. Smith and Leslie Chubb of the Pennsylvania Geological Survey cut the limestone into slabs for insertion and removal from the drains. Field assistance was provided at various times by numerous individuals; Kevin McGonigal is acknowledged for his assistance as an unpaid volunteer. E. I. Robbins identified microbes and G. L. Nord, J. M. Bigham and D. J. Williams identified minerals at the study site. Helpful comments on the study design were provided by K. G. Stollenwerk, and comments on early drafts of this manuscript were provided by several colleagues, including A. W. Rose, R. S. Hedin, G. R. Watzlaf, K. S. Smith, C. J. Lind and two anonymous reviewers. However, the interpretations presented are solely the authors' responsibility.

References

Ali, M.A., Dzombak, D.A., 1996. Interactions of copper, organic acids, and sulfate in goethite suspensions. Geochim. Cosmochim. Acta 60, 5045–5053.

Anderson, M.A., Rubin, A.J. (Eds.), 1981. Adsorption of inorganics at solid-liquid interfaces. Ann Arbor Science Publishers, Inc., Ann Arbor, Mich.

Arakaki, T., Mucci, A., 1995. A continuous and mechanistic representation of calcite reaction-controlled kinetics in dilute solutions at 25°C and 1 Atm total pressure. Aquat. Geochem. 1, 105–130.

Arnold, D.E., 1991. Diversion wells—a low-cost approach to treatment of acid mine drainage. In Proc. of the 12th Annual West Virginia Surface Mine Drainage Task Force Symposium, pp. 39–50. Charleston, West Virginia Mining and Reclamation Association.

Aschenbach, E.T., 1995. An examination of the processes and rates of carbonate dissolution in an artificial acid mine drainage solution. M.S. thesis, Pennsylvania State Univ., University Park, Pa.

Ball, J.W., Nordstrom, D.K., 1991. User's manual for WATEQ4F with revised data base. U.S. Geol. Surv. Open-File Report 91–183.

Benjamin, M.M., Leckie, J.O., 1981. Multiple-site adsorption of Cd, Cu, Zn, and Pb on amorphous iron oxyhydroxides. Journal of Colloid and Interface Science 79, 209–221.

Bigham, J.M., Schwertmann, U., Traina, S.J., Winland, R.L., Wolf, M., 1996. Schwertmannite and the chemical modeling of iron in acid sulfate waters. Geochim. Cosmochim. Acta 60, 2111–2121.

Blowes, D.W., Ptacek, C.J., 1994. Acid-neutralization mechanisms in inactive mine tailings. In: Jambor, J.L., Blowes, D.W. (Eds.), Environmental geochemistry of sulfide mine-wastes 22, 271–292. Mineralogical Association Canada, Short Course Handbook.

Boyer, J., Sarnoski, B., 1995. 1995 progress report—statement of mutual intent strategic plan for the restoration and protection of streams and watersheds polluted by acid mine drainage from abandoned coal mines. Philadelphia, Pa., U.S. Environmental Protection Agency, appendix (http://www.epa.gov/reg3giss/libraryp.htm).

Brady, K.B.C., Perry, E.F., Beam, R.L., Bisko, D.C., Gardner, M.D., Tarantino, J.M., 1994. Evaluation of acid-base accounting to predict the quality of drainage at surface coal mines in Pennsylvania, U.S.A. U.S. Bureau of Mines Special Publication SP 06A, 138–147.

Brady, K.B.C., Rose, A.W., Cravotta, C.A., III, Hellier, W.W., 1997. Bimodal distribution of pH in coal-mine drainage (abs). Geol. Soc. Am., GSA Abstracts with Programs 29(1), 32.

Brant, D.L., Ziemkiewicz, P.F., 1997. Passive removal of manganese from acid mine drainage In Proceedings of the 1997 National Meeting of the American Society for Surface Mining and Reclamation, pp. 741–744. Princeton, W. V., American Society for Surface Mining and Reclamation.

Bricker, O.P., 1965. Some stability relations in the system $Mn–O_2–H_2O$ at 25°C and one atmosphere total pressure. Am. Mineral. 50, 1296–1354.

Brodie, G.A., Britt, C.R., Tomaszewski, T.M., Taylor, H.N., 1991. Use of passive anoxic limestone drains to enhance performance of acid drainage treatment wetlands. In Proc. 1991 National Meeting of the American Society for Surface Mining and Reclamation, 211–228. Princeton, W. V., American Society for Surface Mining and Reclamation.

Coston, J.A., Fuller, C.C., Davis, J.A., 1995. Pb^{2+} and Zn^{2+} adsorption by a natural aluminum- and iron-bearing surface coating on an aquifer sand. Geochim. Cosmochim. Acta 59, 3535–3547.

Cram, J.C., 1996. Diversion well treatment of acid water, Lick Creek, Tioga County, PA. M.S. thesis, Pennsylvania State Univ., University Park, Pa.

Cravotta III, C.A., 1994. Secondary iron-sulfate minerals as sources of sulfate and acidity—the geochemical evolution of acidic ground water at a reclaimed surface coal min in Pennsylvania. In: Alpers, C.N., Blowes, D.W. (Eds.), Environmental geochemistry of sulfide oxidation, pp. 345–364. Washington, D.C. Am. Chem. soc. Symp. Series 550.

Crerar, D.A., Barnes, H.L., 1974. Deposition of deep-sea manganese nodules. Geochim. Cosmochim. Acta 38, 279–300.

Davies, S.H.R., Morgan, J.J., 1989. Manganese(II) oxidation kinetics on metal oxide surfaces. J. Colloid Interface Sci. 129, 63–77.

Ehrlich, H.L., 1990. Geomicrobiology (2nd). Marcel Dekker, Inc., New York.

Ferris, F.G., Tazaki, K., Fyfe, W.S., 1989. Iron oxides in acid mine drainage environments and their association with bacteria. Chem. Geol. 74, 321–330.

Fishman, M.J., Friedman, L. C. (eds.), 1989. Methods for determination of inorganic substances in water and fluvial sediments. U.S. Geological Survey Techniques of Water-Resources Investigations, Book 5, Chapter A1.

Freeze, R.A., Cherry, J.A., 1979. Groundwater. Prentice-Hall, Inc., Englewood Cliffs, N.J.

Hedin, R.S., Watzlaf, G.R., 1994. The effects of anoxic limestone drains on mine water chemistry. U.S. Bureau of Mines Special Publication SP 06A, 185–194.

Hedin, R.S., Nairn, R.W., Kleinmann, R.L.P., 1994a. Passive treatment of coal mine drainage. U.S. Bureau of Mines Information Circular IC 9389.

Hedin, R.S., Watzlaf, G.R., Nairn, R.W., 1994b. Passive treatment of acid mine drainage with limestone. J. Environ. Qual. 23, 1338–1345.

Hem, J.D., 1963. Chemical equilibria and rates of manganese oxidation. U.S. Geol. Surv. Water-Supply Paper 1667–A.

Hem, J.D., 1964. Deposition and solution of manganese oxides. U.S. Geol. Surv. Water-Supply Paper 1667–B.

Hem, J.D., 1977. Reactions of metal ions at surfaces of hydrous iron oxide. Geochim. Cosmochim. Acta 41, 527–538.

Hem, J.D., 1978. Redox processes at surfaces of manganese oxide and their effects on aqueous and metal ions. Chem. Geol. 21, 199–218.

Hem, J.D., Lind, C.J., 1983. Nonequilibrium models for predicting forms of precipitated manganese oxides. Geochim. Cosmochim. Acta 47, 2037–2046.

Hem, J.D., Lind, C.J., 1994. Chemistry of manganese precipitation in Pinal Creek, Arizona, USA—a laboratory study. Geochim. Cosmochim. Acta 58, 1601–1613.

Hill, R.D., Wilmoth, R.C., 1971. Limestone treatment of acid mine drainage. Tans. Soc. Mining Engineers, Soc. Mining Engineers of AIME 250, 162–166.

Kepler, D.A., McCleary, E.C., 1994. Successive alkalinity producing systems (SAP's) for the treatment of acidic mine drainage. U.S. Bureau of Mines Special Publication SP 06A, 195-204.

Kirby, C.S., Elder Brady, J.A., 1998. Field determination of Fe^{2+} oxidation rates in acid mine drainage using a continuously-stirred tank reactor. Appl. Geochem. 13, 509–520.

Kooner, Z.S., 1993. Comparative study of adsorption behavior of copper, lead, and zinc onto goethite in aqueous systems. Environ. Geol. 21, 342–350.

Lind, C.J., Hem, J.D., Roberson, C.E., 1987. Reaction products of manganese-bearing waters. In: Averett, R.C., McKnight, D.M. (Eds.), Chemical quality of water and the hydrologic cycle, pp. 271–301. Chelsea, Michigan, Lewis Publishers, Inc.

Loganathan, P., Burau, R.G., 1973. Sorption of heavy metal ions by a hydrous manganese oxide. Geochim. Cosmochim. Acta 37, 1277–1293.

Lovell, H.L., 1972. Experience with biochemical-iron-oxidation limestone-neutralization process. National Coal Association/Bituminous Coal Research Inc., 4th Symp. Coal Mine Drainage Research, Pittsburgh, Pa.

McKenzie, R.M., 1980. The adsorption of lead and other heavy metals on oxides of manganese and iron. Austral. J. Soil Res. 18, 61–73.

Morse, J.W., 1983. The kinetics of calcium carbonate dissolution and precipitation. In: Reeder, R.J. (Ed.), Carbonates—mineralogy and chemistry, 11, 227–264. Mineral. Soc. Am. Reviews in Mineralogy.

Murad, E., Schwertmann, U., Bigham, J.M., Carlson, L., 1994. Mineralogical characteristics of poorly crystallized precipitates formed by oxidation of Fe^{2+} in acid sulfate waters. In: Alpers, C.N., Blowes, D.W. (Eds.), Environmental geochemistry of sulfide oxidation, pp. 190–200. Washington, D.C., Amer. Chem. Soc. Symp. Series 550.

Nordstrom, D.K., 1977. Thermochemical redox equilibria of Zobell's solution. Geochim. Cosmochim. Acta 41, 1835–1841.

Nordstrom, D.K., Alpers, C.N., 1998. Geochemistry of acid mine waters. In: Plumlee, G.S., Logsdon, M.J. (Eds.), The Environmental Geochemistry of Mineral Deposits–Part A. Processes, methods, and health issues, Vol. 6. Reviews in Econ. Geol.

Plummer, L.N., Parkhurst, D.L., Wigley, M.L., 1979. Critical review of the kinetics of calcite dissolution and precipitation. In: Jenne, E.A. (Ed.), Chemical modeling in aqueous systems—Speciation, sorption, solubility, and kinetics, pp. 537–573. Am. Chem. Soc. Symp. Series 93.

Powell, J.D., 1988. Origin and influence of coal mine drainage on streams of the United States. Environ. Geol. Water Sci. 11, 141–152.

Robbins, E.I., Cravotta III, C.A., Savela, C.E., Nord, G.L., Jr., Balciauskas, K.A., Belkin, H.E., 1997. Hydrobiogeochemical interactions on calcite and gypsum in "anoxic" limestone drains in West Virginia and Pennsylvania. In 1997 International Ash Utilization Symposium, pp. 546–559. Univ. Kentucky, Lexington, Ky. (http://energy.er.usgs.gov/products/papers/iaus_97/).

Robbins, E.I., D'Agostino, J.P., Ostwald, J., Fanning, D.S., Carter, V., Van Hoven, R.L., 1992. Manganese nodules and microbial oxidation of manganese in the Huntley Meadows wetland, Virginia, USA. In: Skinner, H.C.W., Fitzpatrick, R.W. (Eds.), Biomineralization processes of iron and manganese—modern and ancient environments. Catena Suppl. 21, 179–202.

Robbins, E.I., Nord, G.L., Savela, C.E., Eddy, J.I., Livi, K.J.T., Gullett, C.D., Nordstrom, D.K., Chou, I.-M., Briggs, K.M., 1996. Microbial and mineralogical analysis of aluminum-rich precipitates that occlude porosity in a failed anoxic limestone drain, Monongalia County, West Virginia. In: Chiang, S-H. (Ed.), Coal-energy and the environment, 2, 761–767. Proc. 13th Ann. Internat. Pittsburgh Coal Conference.

Rose, A.W., Cravotta III, C.A., 1998. Geochemistry of coal-mine drainage. In: Smith, M.W., Brady, K.B.C. (Eds.), The prediction and prevention of acid drainage from surface coal mines in Pennsylvania, Chap. 1. Harrisburg, Pennsylvania Department of Environmental Protection.

Rose, S., Ghazi, A.M., 1997. Release of sorbed sulfate from iron oxyhydroxides precipitated from acid mine drainage associated with coal mining. Environ. Sci. Technol. 31, 2136–2140.

Smith, K.S., Ranville, J.R., Plumlee, G.S., Macalady, D.L., 1998. Predictive double-layer modeling of metal sorption in mine-drainage systems. In: Jenne, E.A. (Ed.), Metal adsorption by geomedia. San Diego, Academic Press.

Sterner, P.L., Skousen, J.G., Donovan, J.J., 1998. Geochemistry of laboratory anoxic limestone drains. In Proc. 1998 National Meeting of the American Society for Surface Mining and Reclamation, pp. 214–234. Princeton, W. V., American Society for Surface Mining and Reclamation.

Stumm, W., Morgan, J.J., 1996. Aquatic chemistry—chemical equilibria and rates in natural waters (3rd). Wiley-Interscience, New York.

Stumm, W., Sulzberger, B., 1992. The cycling of iron in natural environments—considerations based on laboratory studies of heterogeneous redox processes. Geochim. Cosmochim. Acta 56, 3233–3257.

Tamura, H., Goto, K., Nagayama, M., 1976. The effect of ferric hydroxide in the oxygenation of ferrous ions in neutral solutions. Corros. Sci. 16, 197–207.

Taylor, R.M., Schwertmann, U., 1978. The influence of aluminum on iron oxides. Part I. The influence of Al on Fe oxide formation from the Fe(II) system. Clays Clay Minerals 26, 373–383.

Turner, D., McCoy, D., 1990. Anoxic alkaline drain treatment system, a low cost acid mine drainage treatment alternative. In: Graves, D.H., DeVore, R.W. (Eds.), 1990 Symp. Surface Mining Hydrology, Sedimentology and Reclamation, 73–75. Univ. Kentucky, Lexington, Ky.

Watzlaf, G.R., 1997. Passive treatment of acid mine drainage in down-flow limestone systems. In Proc. 1997 National Meeting American Society for Surface Mining and Reclamation, pp. 611–622. Princeton, W. V., American Society for Surface Mining and Reclamation.

Watzlaf, G.R., Kleinhenz, J.W., Odoski, J.R., Hedin, R.S., 1994. The performance of the Jennings Environmental Center anoxic limestone drain (abs). U.S. Bureau Mines Spec. Publ. SP 06B.

Watzlaf, G.R., Nairn, R.W., Hedin, R.S., Cooper, A.R., Borek, S.L., 1992. A laboratory investigation of the effect of Fe^{2+}, Fe^{3+} and Al^{3+} on the performance of anoxic limestone drains (abs). In Proc. 13th Annual Meeting West Virginia Surface Mine Drainage Task Force. West Virginia University, Morgantown, W. Va.

Webster, J.G., Swedlund, P.J., Webster, K.S., 1998. Trace metal adsorption onto an acid mine drainage iron(III) oxy hydroxy sulfate. Environ. Sci. Technol. 32, 1361–1368.

Williamson, M. A., Kirby, C. S., Rimstidt, J. D., 1992. The kinetics of iron oxidation in acid mine drainage (abs). In V. M. Goldschmidt Conference Program and Abstracts. The Geochemical Society, University Park, Pa., A–121.

Wood, C. R., 1996. Water quality of large discharges from mines in the anthracite region of eastern Pennsylvania. U.S. Geol. Surv. Water-Resour. Investigations Rep. 95–4243.

Wood, W. W., 1976. Guidelines for the collection and field analysis of ground-water samples for selected unstable constituents. U.S. Geol. Surv. Techniques of Water Res. Investigations, Book 1, Chap. D2.

Zachara, J.M., Cowan, C.E., Resch, C.T., 1991. Sorption of divalent metals on calcite. Geochim. Cosmochim. Acta 55, 1549–1562.

Ziemkiewicz, P.F., Skousen, J.G., Brant, D.L., Sterner, P.L., Lovett, R.J., 1997. Acid mine drainage treatment with armored limestone in open limestone channels. J. Environ. Qual. 26, 1017–1024.